Pendellösung Interferometry as a Probe for New Interactions

Benjamin Heacock
NIST

PSI Workshop
October 22, 2019

National Institute of Standards and Technology
U.S. Department of Commerce

NC STATE UNIVERSITY

Overview

Pendellosung Interferometry

- Precise measurements of neutron-crystalline structure factors

Physics contained in crystalline structure factors

- Thermal vibrations, neutron charge radius, BSM force mediators

What can precision measurements (relative unc ~5 x 10^{-5}) of neutron-silicon structure factors achieve?

Experiment

Preliminary Results

Pendellösung - Bragg scattering as a two-state system

$$\vec{Q} = \vec{H}$$

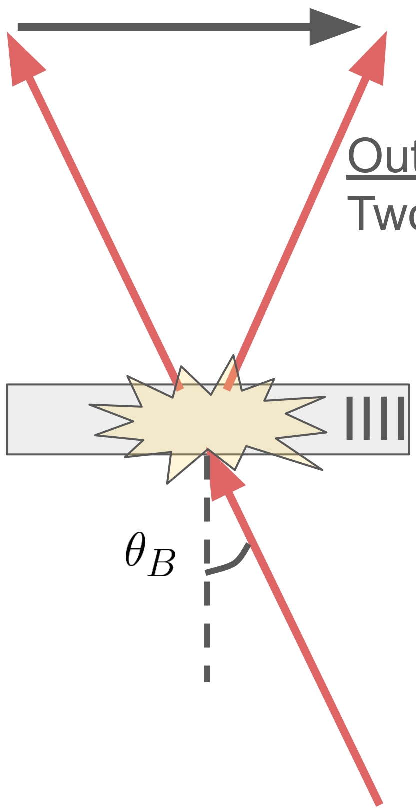

Momentum Transfer:
Set by Bragg plane spacing

$$H = \frac{2\pi}{d} = \frac{2\pi}{a}\sqrt{h^2 + l^2 + k^2}$$

Outside the crystal:
Two free neutron states

$$\mathcal{H} = \frac{\hbar^2}{2m}\begin{pmatrix} K^2 + v_0 & v_H \\ v_{-H} & K_H^2 + v_0 \end{pmatrix}$$

$$\vec{K}_H = \vec{K} + \vec{H}$$

Inside the crystal:
Two states
Linear combinations of external states
Each state sees separate index of refractions
Same total energy, differing kinetic terms
Pendellosung is the interference between two internal states

Measuring Pendellosung

Change wavelength using Bragg's law in a collimated white beam

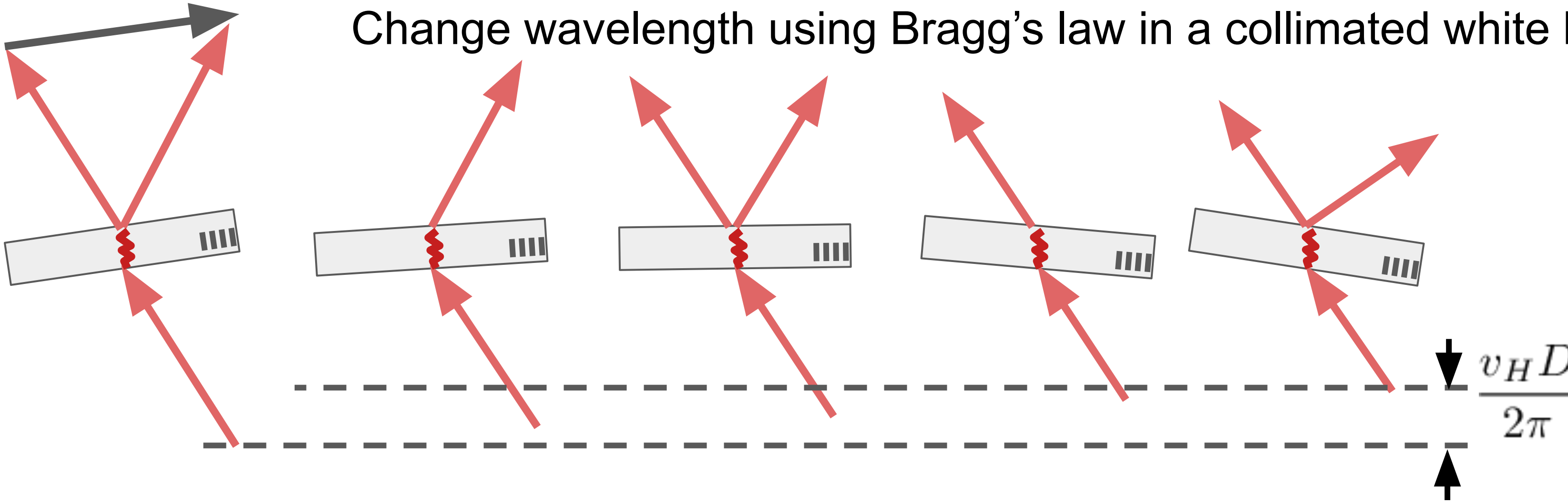

Change optical thickness by tilting crystal about H-axis

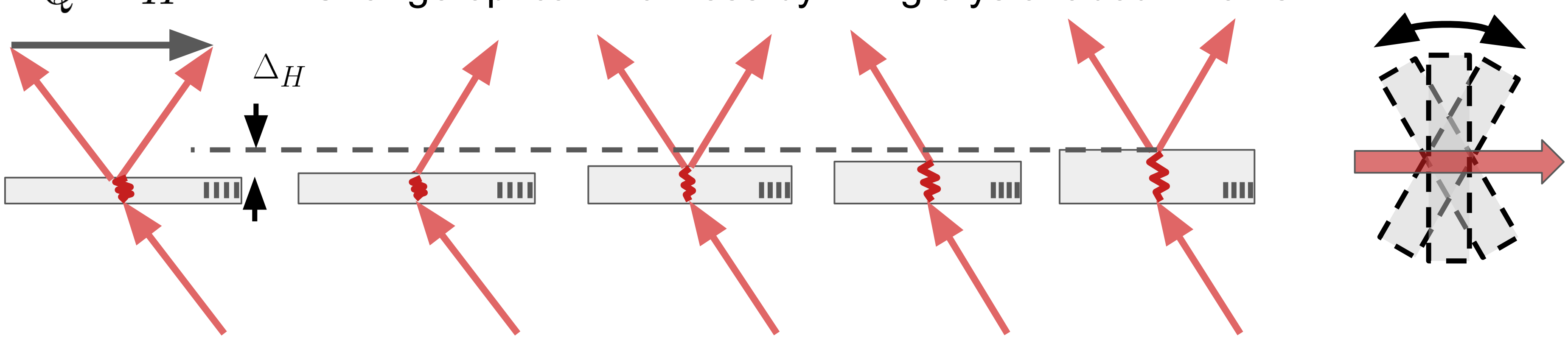

Measuring Pendellosung

<u>In Summary</u>: By rotating a crystal in a carefully-prepared neutron beam, the phase of the oscillations between the diffracted and transmitted beams provides a precise measure of the neutron-crystalline potential.

OBSERVATION OF PENDELLÖSUNG FRINGE STRUCTURE IN NEUTRON DIFFRACTION*

C. G. Shull
Brookhaven National Laboratory, Upton, New York,
and Massachusetts Institute of Technology, Cambridge, Massachusetts
(Received 26 August 1968)

Spherical-Wave Neutron Propagation and Pendellösung Fringe Structure in Silicon*

C. G. Shull and J. A. Oberteuffer
Massachusetts Institute of Technology, Cambridge, Massachusetts 02139
(Received 11 August 1972)

Neutron Pendellösung Fringe Structure in the Laue Diffraction by Germanium *

C. G. Shull and W. M. Shaw
Massachusetts Institute of Technology, Cambridge, Massachusetts, USA
(Z. Naturforsch. **28** a, 657—661 [1973] ; received 22 January 1973)

Dedicated to Gerhard Borrmann on his 65th birthday

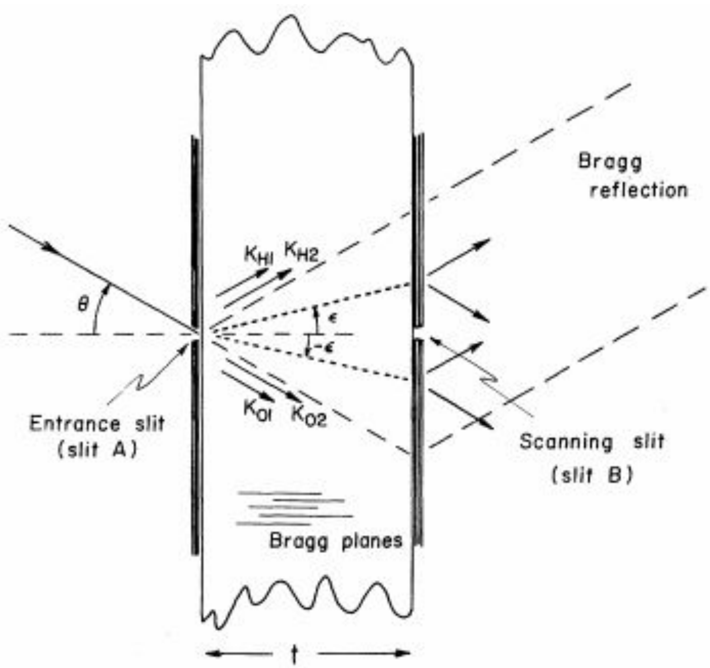

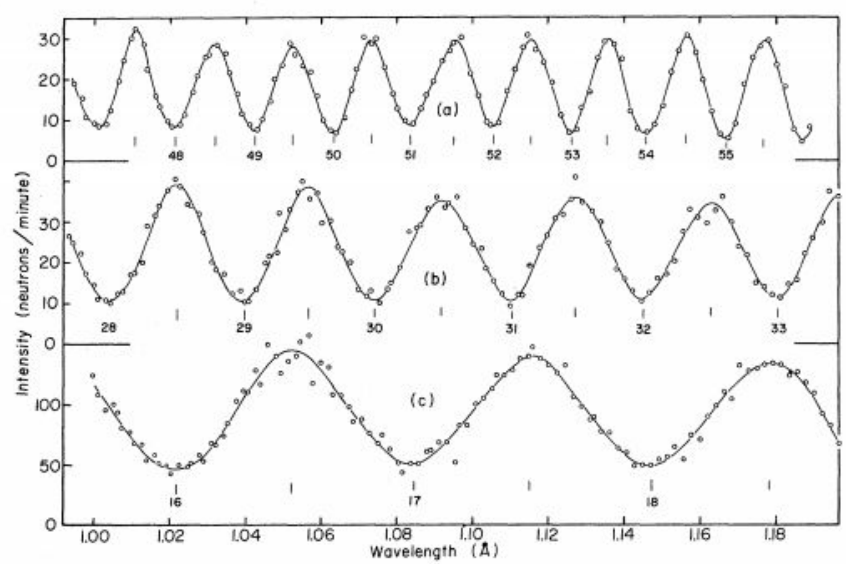

Pendellosung Phase Shift

Crystal structure factors

- Fourier transform of the crystalline potential evaluated at Q=H
- Sensitive to physics on the atomic scale, including new physics → **BSM Force Mediator**
- Probes atomic charge densities → **Neutron Charge Radius**, Schwinger scattering, nEDM

Crystalline Symmetry - Phase shift for each scattering center

- Interference between scattering centers causes selection rules (forbidden reflections) and highly suppressed Schwinger scattering and nEDM terms for centrosymmetric crystals
- Averaging the phases over thermal vibrations → **Debye Waller Factor**

Pendellosung Phase Shift

VV Fedorov, Poster 40: Neutron spin rotation at Laue diffraction in a weakly deformed transparent noncentrosymmetric crystal

Crystal structure factors

- Fourier transform of the crystalline potential evaluated at Q=H
- Sensitive to physics on the atomic scale, including new physics → **BSM Force Mediator**
- Probes atomic charge densities → **Neutron Charge Radius**, Schwinger scattering, nEDM

Crystalline Symmetry - Phase shift for each scattering center

- Interference between scattering centers causes selection rules (forbidden reflections) and highly suppressed Schwinger scattering and nEDM terms for centrosymmetric crystals
- Averaging the phases over thermal vibrations → **Debye Waller Factor**

Crystal Structure Factor

Neutron-atom interaction

Thermal smearing

$$v_H = \frac{2m}{a^3}\widetilde{V}(H)\left\langle \sum_v e^{i\vec{H}\cdot\vec{x}_v} \right\rangle$$

Debye-Waller Factor

Charge Radius (div E)

New Forces

$$v_H = \left(\frac{4\pi}{a^3}\sum_v e^{i\vec{H}\cdot\vec{x}_v}\right)\underbrace{\left\{e^{-W}\left[b_N - [Z - f_e(H)]b_{\mathrm{ne}} + b_5(H)\right]\right\}}_{b(H)}$$

Debye-Waller Factor

Mean-square displacement matrix takes on a simple form for centrosymmetric crystals

$$\left\langle e^{i\vec{H}\cdot\vec{u}} \right\rangle = e^{-\frac{1}{2}\vec{H}\cdot U\cdot\vec{H}}$$

$$U_{ij} = \frac{1}{3}\langle u^2\rangle\delta_{i,j}$$

$$\left\langle e^{i\vec{H}\cdot\vec{u}} \right\rangle = e^{-W} = \exp\left[-\frac{1}{16\pi^2}BH^2\right]$$

Neutron Charge Radius

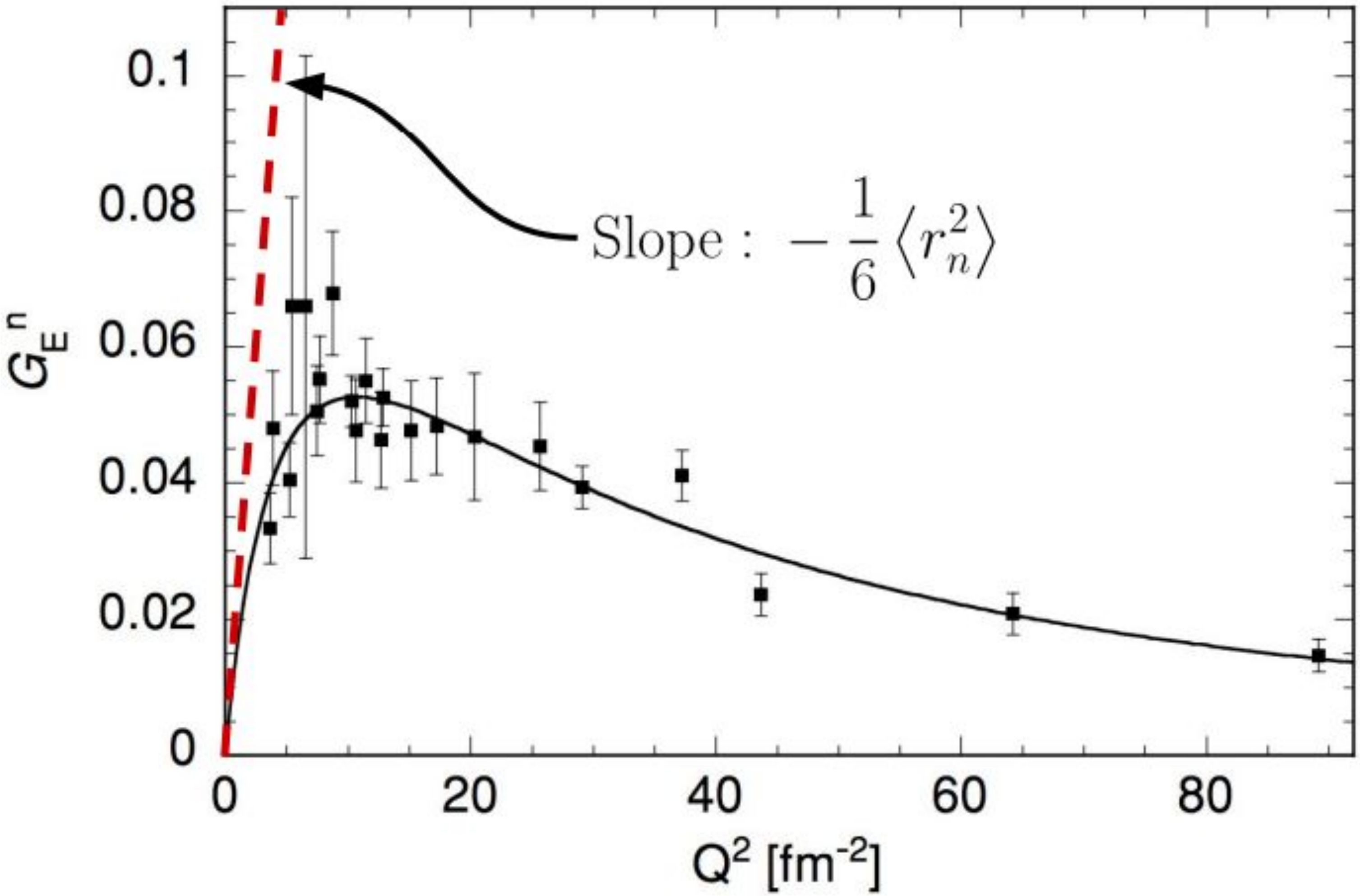

Gentile & Crawford 2011

PHYSICAL REVIEW C **66**, 055210 (2002)

Neutron charge radius deduced from Bragg reflection technique

J.-M. Sparenberg* and H. Leeb
Atominstitut der Österreichischen Universitäten, Technische Universität Wien, Wiedner Hauptstraße 8-10, A-1040 Vienna, Austria
(Received 16 January 2002; published 27 November 2002)

The possibility of the determination of the neutron mean square charge radius from high-precision thermal-neutron measurements of the nuclear scattering length and of the scattering amplitudes of Bragg reflections is considered. Making use of the same Pendellösung technique as Shull [Phys. Rev. Lett. **21**, 1585 (1968)], the scattering amplitudes of about eight higher-order Bragg reflections in silicon could be measured without single-scattering contamination. This would provide a value of the neutron charge radius as precise as the disagreeing Argonne-Garching and Dubna values, as well as a Debye-Waller factor of silicon ten times more precise than presently available.

DOI: 10.1103/PhysRevC.66.055210 PACS number(s): 14.20.Dh, 03.75.Dg, 13.60.Fz, 28.20.Cz

hkl	$f_{x\text{-ray}}$	b(Q)/b(0)-1
111	10.6298(5)	-0.01094(20)
220	8.4179(6)	
311	7.7134(10)	
400	7.0293(4)	
331	6.7571(9)	
⋮	⋮	
880	1.5514(18)	

PDG Values

n MEAN-SQUARE CHARGE RADIUS

The mean-square charge radius of the neutron, $\langle r_n^2 \rangle$, is related to the neutron-electron scattering length b_{ne} by $\langle r_n^2 \rangle = 3(m_e a_0/m_n) b_{ne}$, where m_e and m_n are the masses of the electron and neutron, and a_0 is the Bohr radius. Numerically, $\langle r_n^2 \rangle = 86.34\ b_{ne}$, if we use a_0 for a nucleus with infinite mass.

VALUE (fm^2)		*DOCUMENT ID*		*COMMENT*
$-$0.1161$\pm$0.0022 OUR AVERAGE				Error includes scale factor of 1.3. See the ideogram below.
$-0.115 \pm 0.002 \pm 0.003$		KOPECKY	97	ne scattering (Pb)
$-0.124 \pm 0.003 \pm 0.005$		KOPECKY	97	ne scattering (Bi)
-0.114 ± 0.003		KOESTER	95	ne scattering (Pb, Bi)
-0.134 ± 0.009		ALEKSANDR...	86	ne scattering (Bi)
-0.115 ± 0.003	[20]	KROHN	73	ne scattering (Ne, Ar, Kr, Xe)
• • • We do not use the following data for averages, fits, limits, etc. • • •				
$-0.117\ ^{+0.007}_{-0.011}$		BELUSHKIN	07	Dispersion analysis
$-0.113 \pm 0.003 \pm 0.004$		KOPECKY	95	ne scattering (Pb)
-0.114 ± 0.003		KOESTER	86	ne scattering (Pb, Bi)
-0.118 ± 0.002		KOESTER	76	ne scattering (Pb)
-0.120 ± 0.002		KOESTER	76	ne scattering (Bi)
-0.116 ± 0.003		KROHN	66	ne scattering (Ne, Ar, Kr, Xe)

[20] This value is as corrected by KOESTER 76.

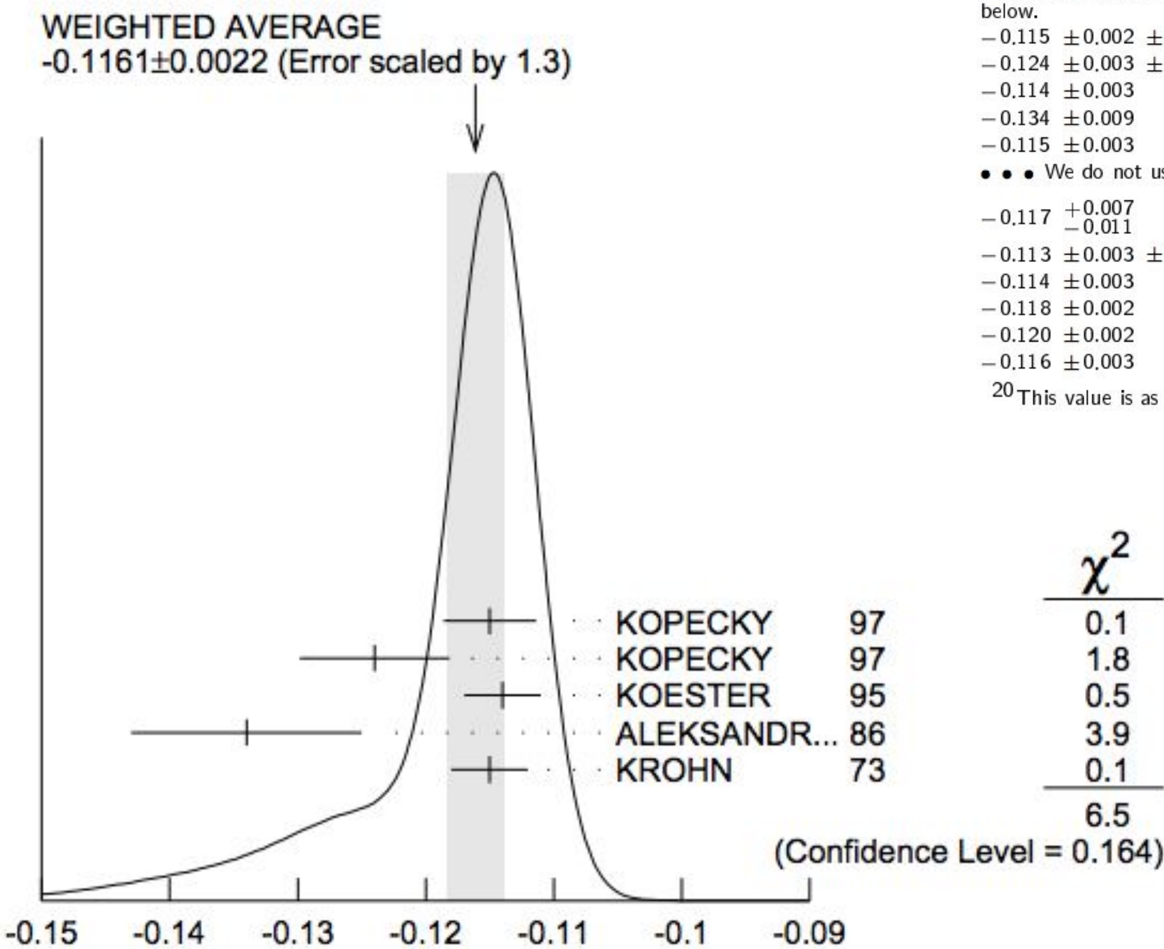

n mean-square charge radius

x-ray form factor

$$[Z - f_e(Q)]\, b_{\rm ne}$$

$$b_{\rm ne} = \frac{\langle r_n^2 \rangle}{86.34\ \text{fm}}$$

PHYSICAL REVIEW C **75**, 015501 (2007)

Neutron interferometric method to provide improved constraints on non-Newtonian gravity at the nanometer scale

Geoffrey L. Greene

Department of Physics, University of Tennessee, Knoxville, Tennessee 37996, USA and Physics Division, Oak Ridge National Laboratory, Oak Ridge, Tennessee 37831, USA

Vladimir Gudkov

Department of Physics and Astronomy, University of South Carolina, Columbia, South Carolina 29208, USA

(Received 31 August 2006; published 4 January 2007)

In recent years, an energetic experimental program has set quite stringent limits on a possible "non-$1/r^2$" dependence on gravity at short length scales. This effort has been largely driven by the predictions of theories based on compactification of extra spatial dimensions. It is characteristic of many such theories that the strength and length scales of such anomalous gravity are not clearly determined from first principles. As a result, it is productive to extend the current limits the range and strength of such hypothetical interactions. As a heavy, neutral, and (almost) stable particle, the neutron provides an ideal probe for the study of such hypothetical interactions at very short range. In this work, we describe methods based on neutron interferometry which have the capability to provide improved sensitivity non-Newtonian forces down to length scales at and below an nanometer.

Theoretical Motivations for Short-Range Forces

- General Relativity (GR) is non-renormalizable
  - It breaks down at high energies
  - Weakest of four forces and very high energies → Difficult to measure
  - Gravitational phenomena has never been measured at a length scale less than 10 μm
- Some theories that provide an ultraviolet (UV) completion to GR also predict short range forces
  - Perturbations to gravity at less than 100 μm
  - Many theories → wide parameter space to constrain
- Other new physics predict new short range forces
  - Light Dark Matter (Fayet 2007)
  - Dark Energy (Zee 2004)
  - Neutrino Masses (Arkani-Hamed & Dimopoulos 2002)

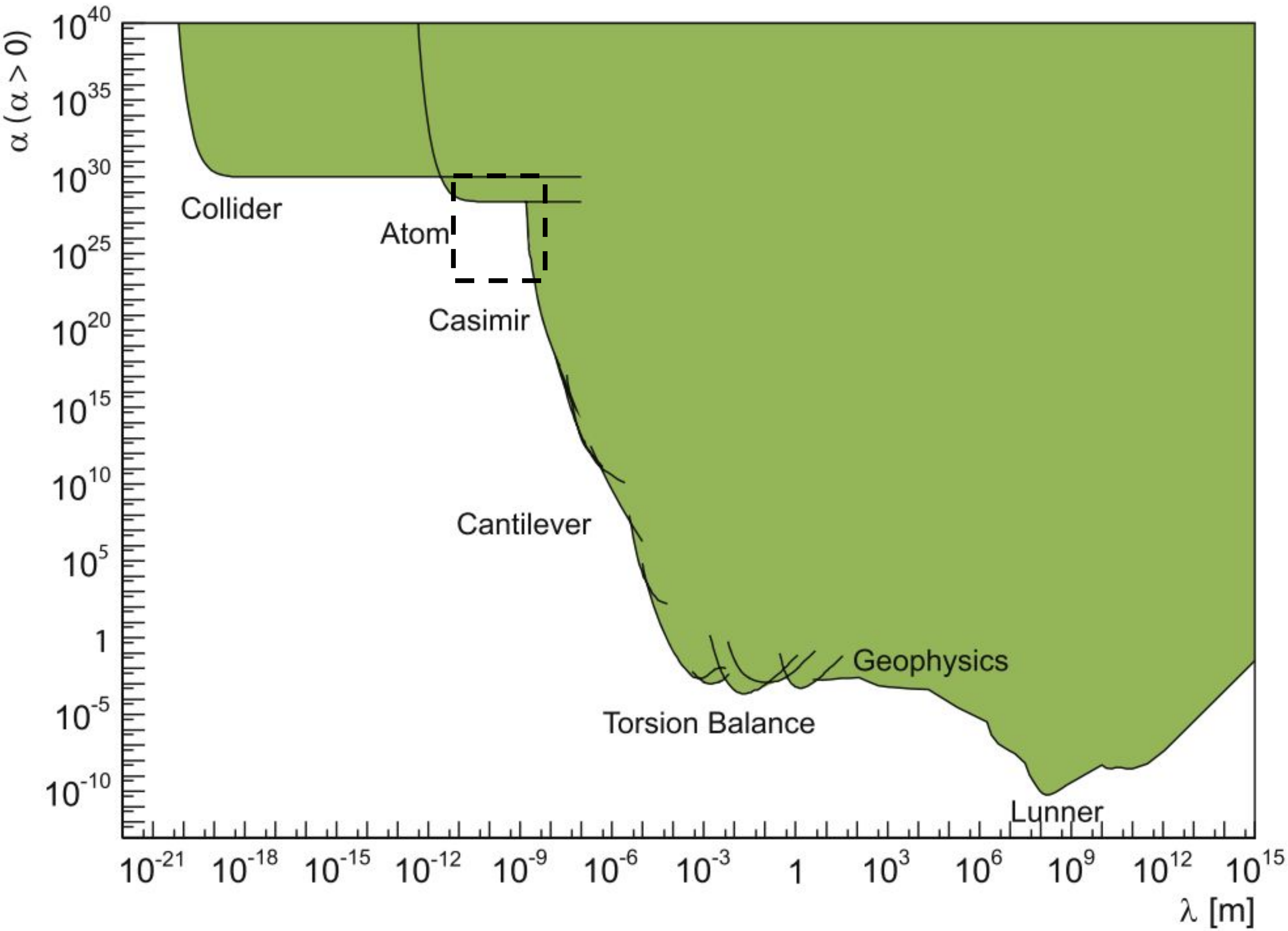

Murata & Tanaka 2015

New Forces

Yukawa (Most Common)

$$V = -G\frac{m_1 m_2}{r}\left[1 + \alpha e^{-r/\lambda}\right]$$

$$b_5(Q) = -\frac{m}{2\pi} g^2 Q_n Q_N \frac{\lambda_5^2}{1 + Q^2\lambda^2} = \alpha_G 2Gm^2 M\left(\frac{\lambda_5^2}{1 + Q^2\lambda_5^2}\right)$$

$$\boxed{b_5(Q) = -1.6 \times 10^{-26}\alpha_G \frac{\lambda_5^2}{1 + Q^2\lambda_5^2}}$$ (Silicon)

Power Law Arkani-Hamed, Dimopoulos, and Dvali (ADD)

$$V = -G\frac{m_1 m_2}{r}\left[1 + \left(\frac{\lambda}{r}\right)^n\right]$$

$$b(Q) = \exp\left[-\frac{1}{16\pi^2}BQ^2\right]\left\{b_N - \left[Z - f_e(Q)\right]b_{\mathrm{ne}} + b_5(Q)\right\}$$

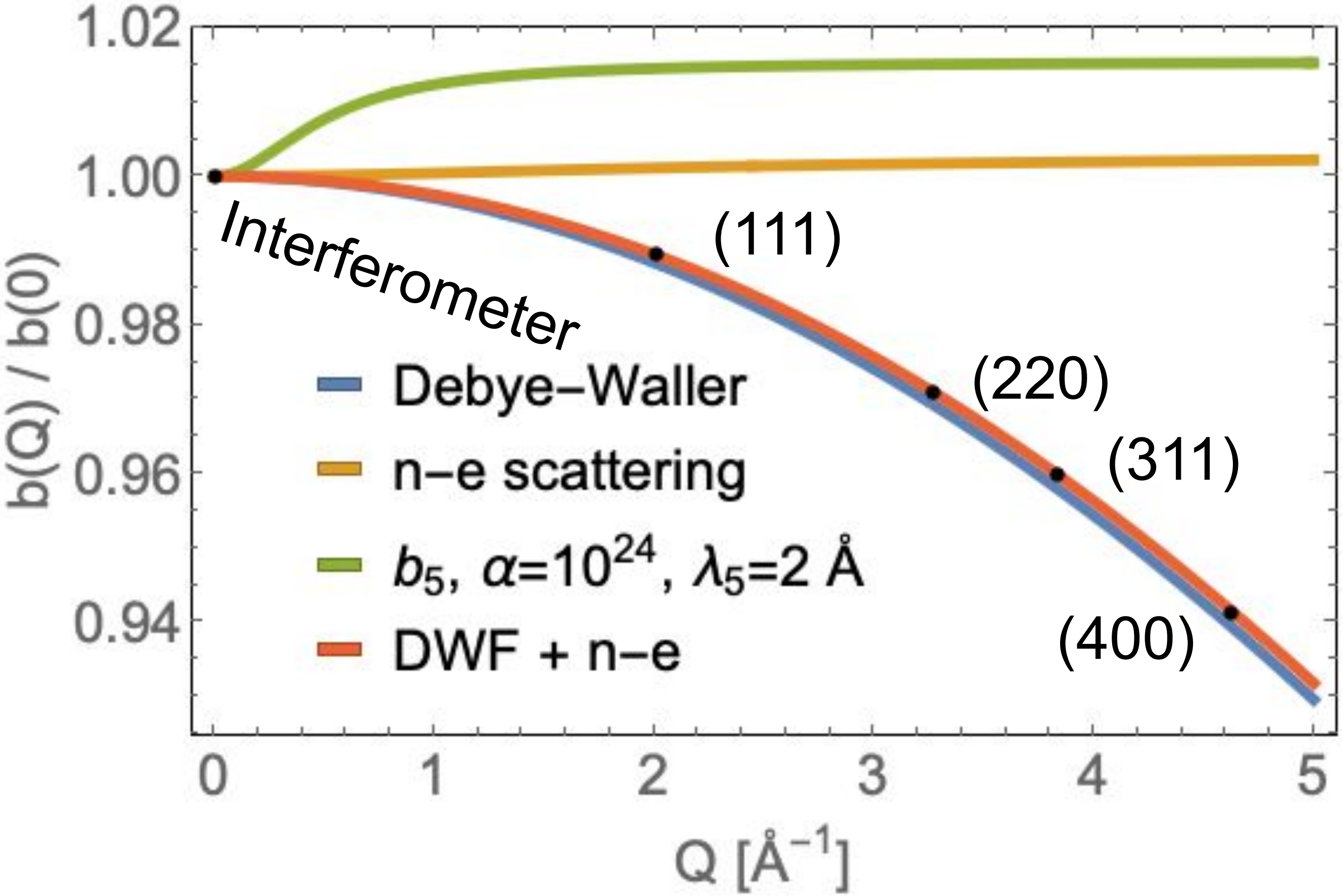

NIST Center for Neutron Research

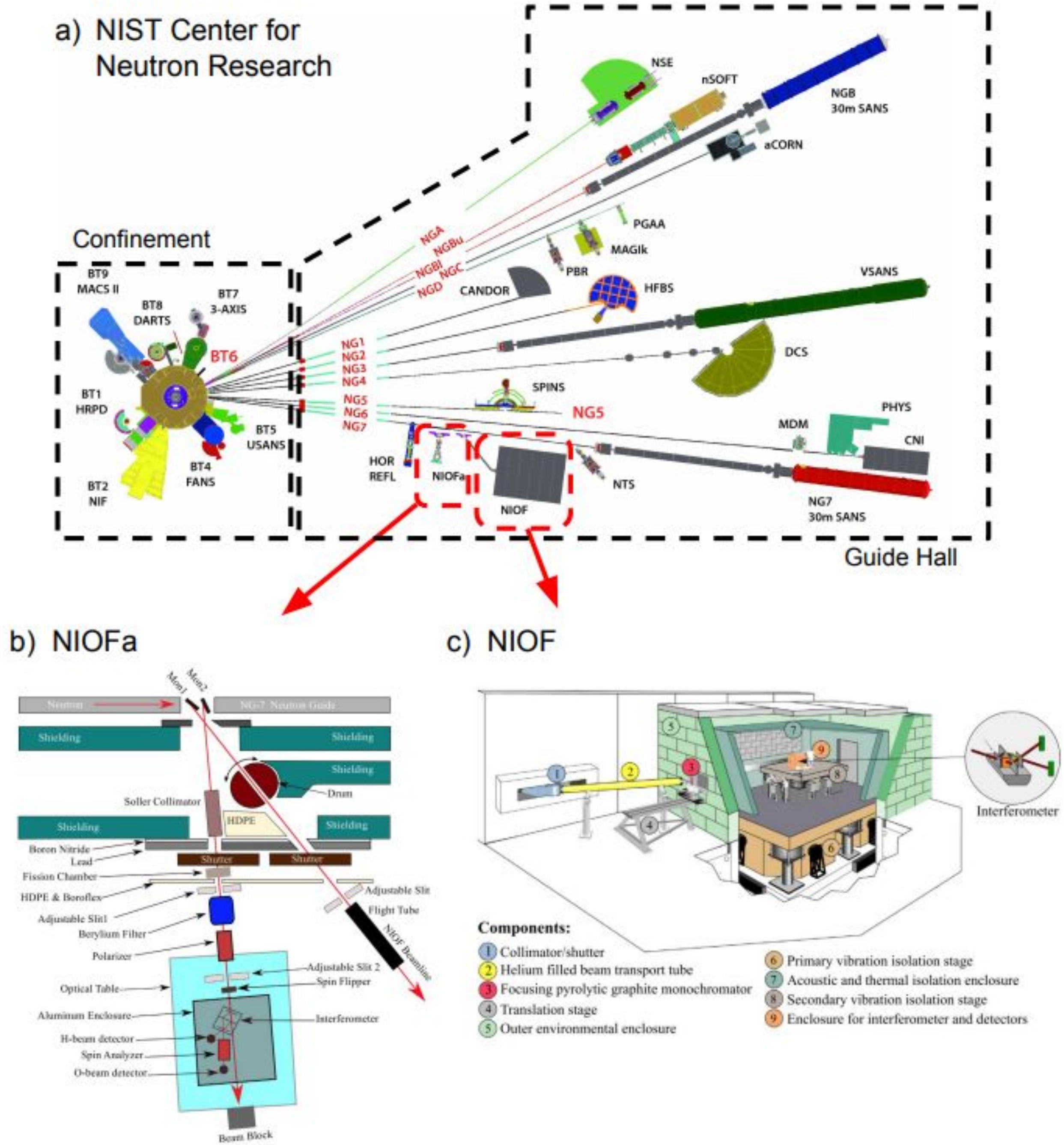
a) NIST Center for Neutron Research
Confinement
Guide Hall
BT9
MACS II
BT8
DARTS
BT7
3-AXIS
BT6
BT1
HRPD
BT5
USANS
BT4
FANS
BT2
NIF
NSE
nSOFT
NGB
30m SANS
aCORN
PGAA
MAGIk
PBR
CANDOR
HFBS
VSANS
DCS
SPINS
NG5
PHYS
MDM
CNI
HOR
REFL
NIOFa
NIOF
NTS
NG7
30m SANS
NGA
NGBu
NGBl
NGC
NGD
NG1
NG2
NG3
NG4
NG5
NG6
NG7
b) NIOFa
Mon1
Mon2
Neutron
NG-7 Neutron Guide
Shielding
Shielding
Shielding
Drum
Soller Collimator
HDPE
Shielding
Shielding
Boron Nitride
Lead
Shutter
Shutter
Fission Chamber
HDPE & Boroflex
Adjustable Slit
Flight Tube
Adjustable Slit1
Beryllium Filter
NIOF Beamline
Polarizer
Adjustable Slit 2
Spin Flipper
Optical Table
Aluminum Enclosure
Interferometer
H-beam detector
Spin Analyzer
O-beam detector
Beam Block
c) NIOF
Interferometer
Components:
1 Collimator/shutter
2 Helium filled beam transport tube
3 Focusing pyrolytic graphite monochromator
4 Translation stage
5 Outer environmental enclosure
6 Primary vibration isolation stage
7 Acoustic and thermal isolation enclosure
8 Secondary vibration isolation stage
9 Enclosure for interferometer and detectors

Experiment

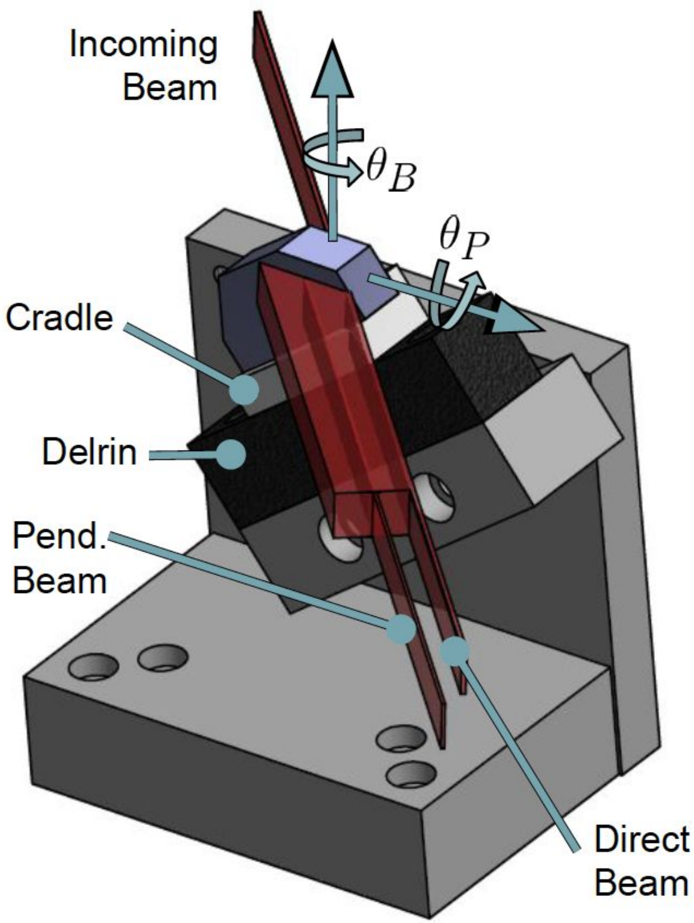

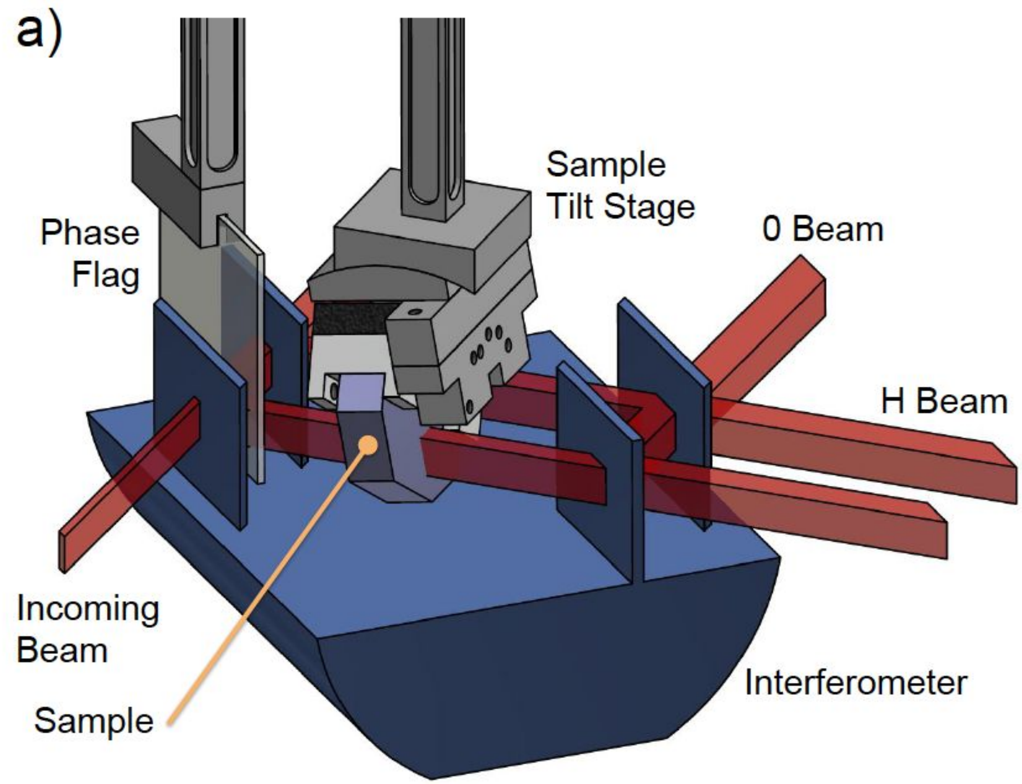

Measure *D b(H)*

Measure *D b(0)*

Strain and Crystal Thickness

Measured phase shift is proportional to crystal thickness

Strain gradients cause wavelength-dependent shift in the pendellosung fringe position

Previous measurements showed large strain gradients (~100 nrad mm^{-1})

> This level of strain is (relatively) large compared to experience with interferometers

Required crystal flatness is at odds with need to chemically etch

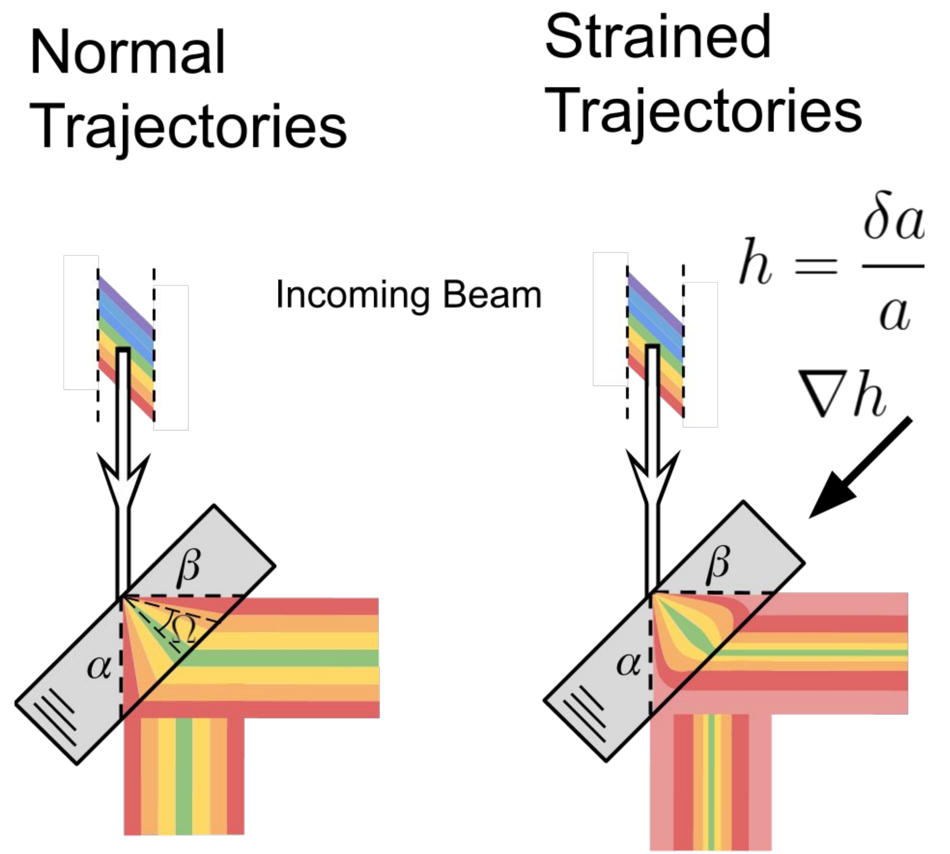

Strain and Crystal Thickness

Measured phase shift is proportional to crystal thickness

Strain gradients cause wavelength-dependent shift in the pendellosung fringe position

Previous measurements showed large strain gradients (~100 nrad mm^{-1})

> This level of strain is (relatively) large compared to experience with interferometers

Required crystal flatness is at odds with need to chemically etch

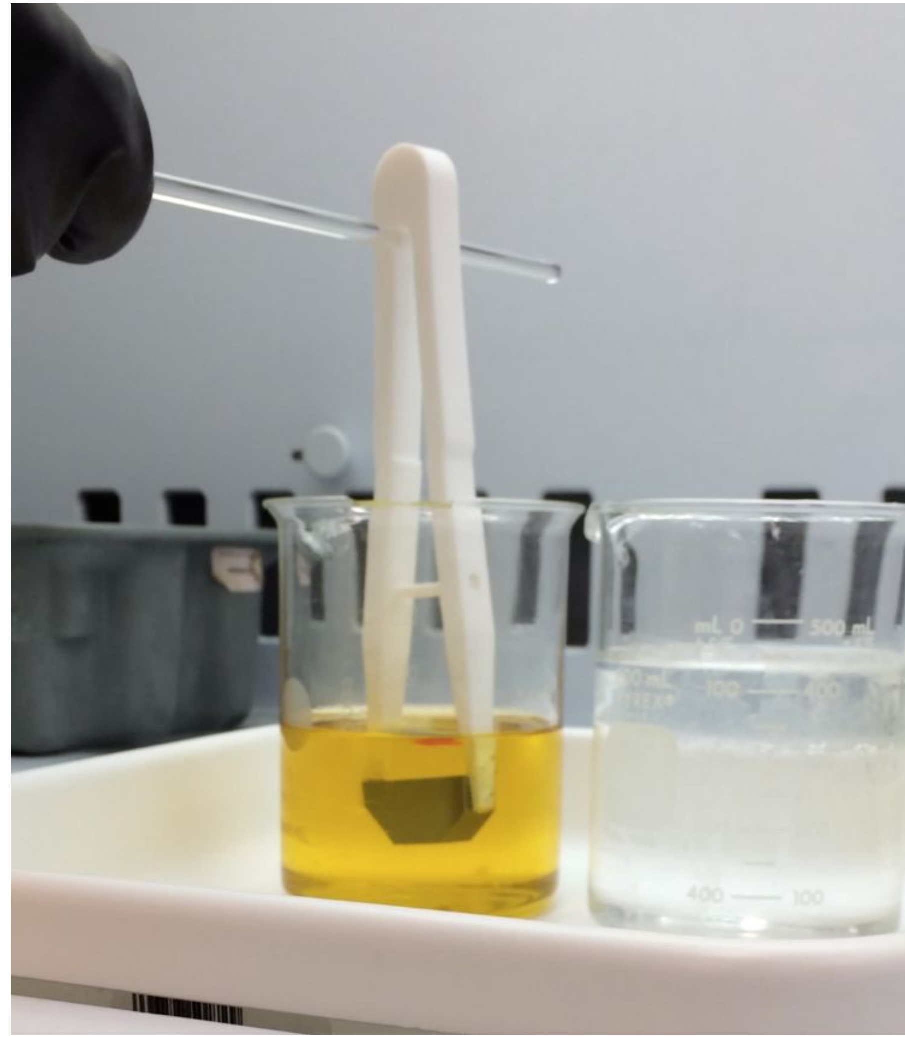

Strain and Crystal Thickness

Interferometer	**Condition**	**∇h** (10^{-9} mm^{-1})
Skew	Etched (>30 um)	4
“Thin Blade”	Etched (>30 um)	5
	Annealed	1
Two-Blade	Precision Machined	$>10^4$
	Annealed	8
	Etched (4 um)	0.2
Shull	“Polished”	100

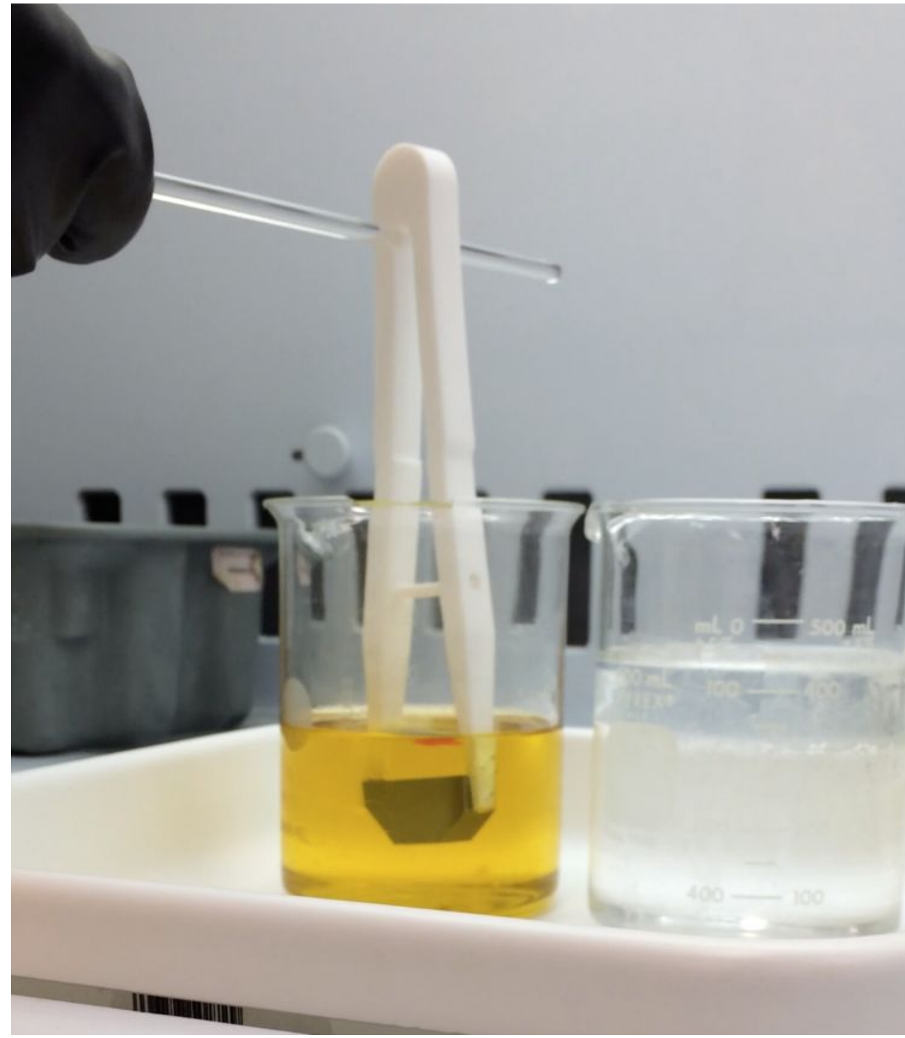

Interferometer Inspiration

- Sparenburg & Leeb 2003: - Pendellosung for multiple Q^2
- Wietfeldt et al. 2006*: Diffracting crystal rotating in an interferometer
- ILL Two Loop Interferometer*

*Relies on dynamical phase contributions from (twisted) interferometers

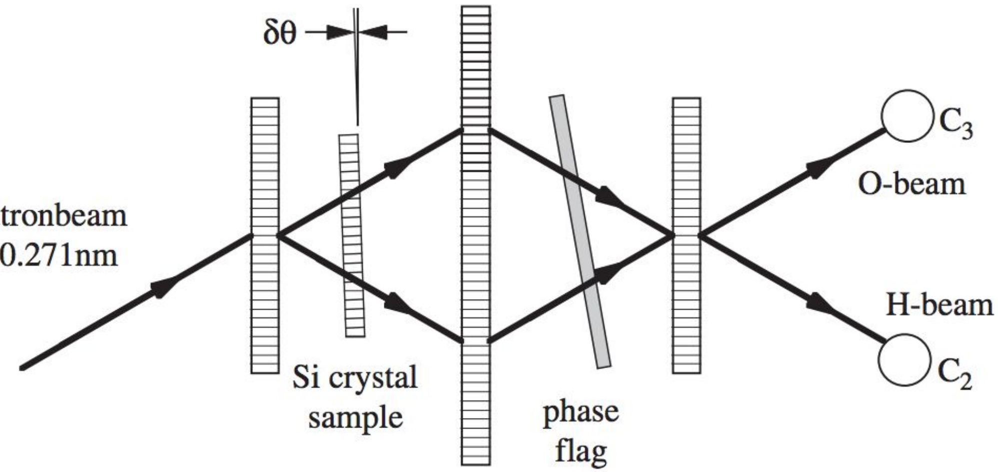

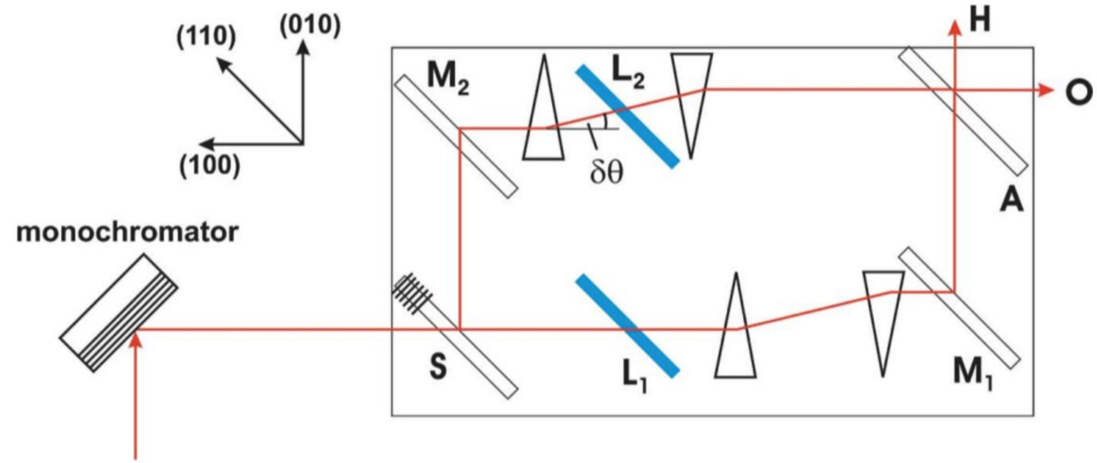

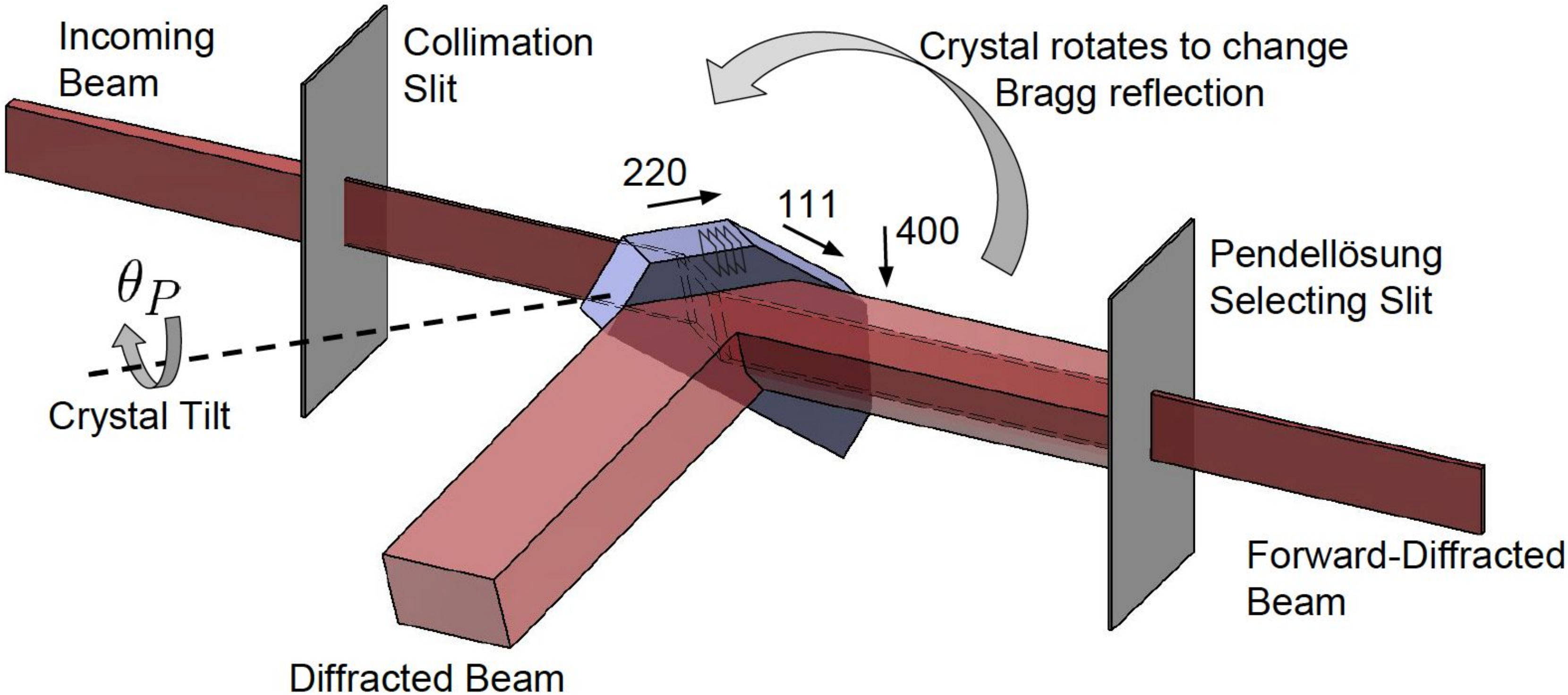
Incoming
Beam
Collimation
Slit
Crystal rotates to change
Bragg reflection
220
111
400
θ_P
Crystal Tilt
Pendellösung
Selecting Slit
Forward-Diffracted
Beam
Diffracted Beam

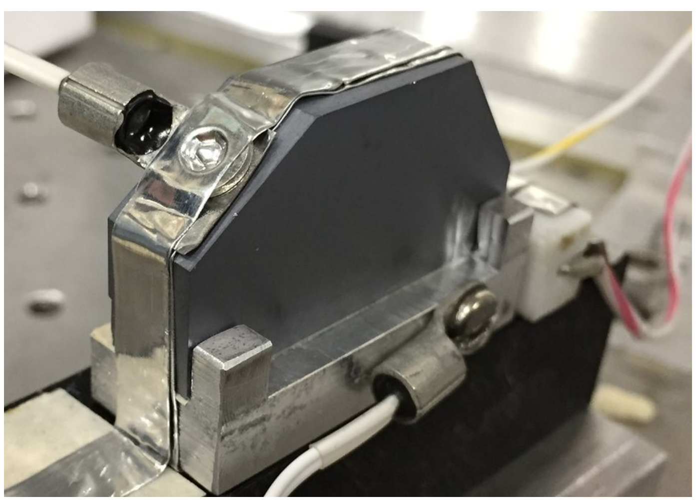

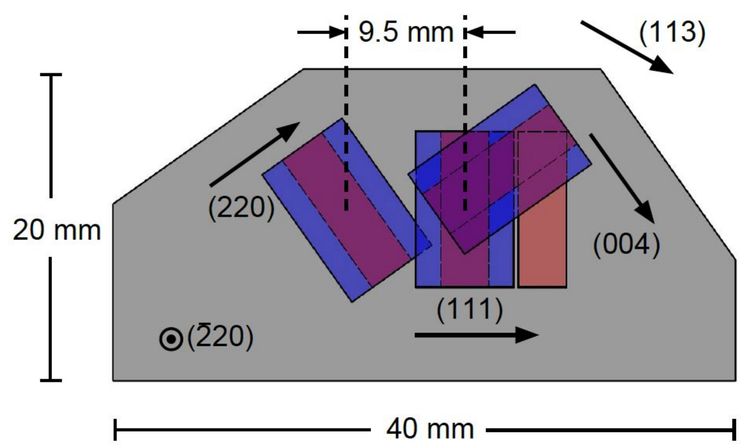
9.5 mm
(113)
20 mm
(220)
(004)
(111)
$\odot(\bar{2}20)$
40 mm

Heater

Heater control probe

Crystal

Temperature Probes

Mounting holes for each reflection

Double tilt stages

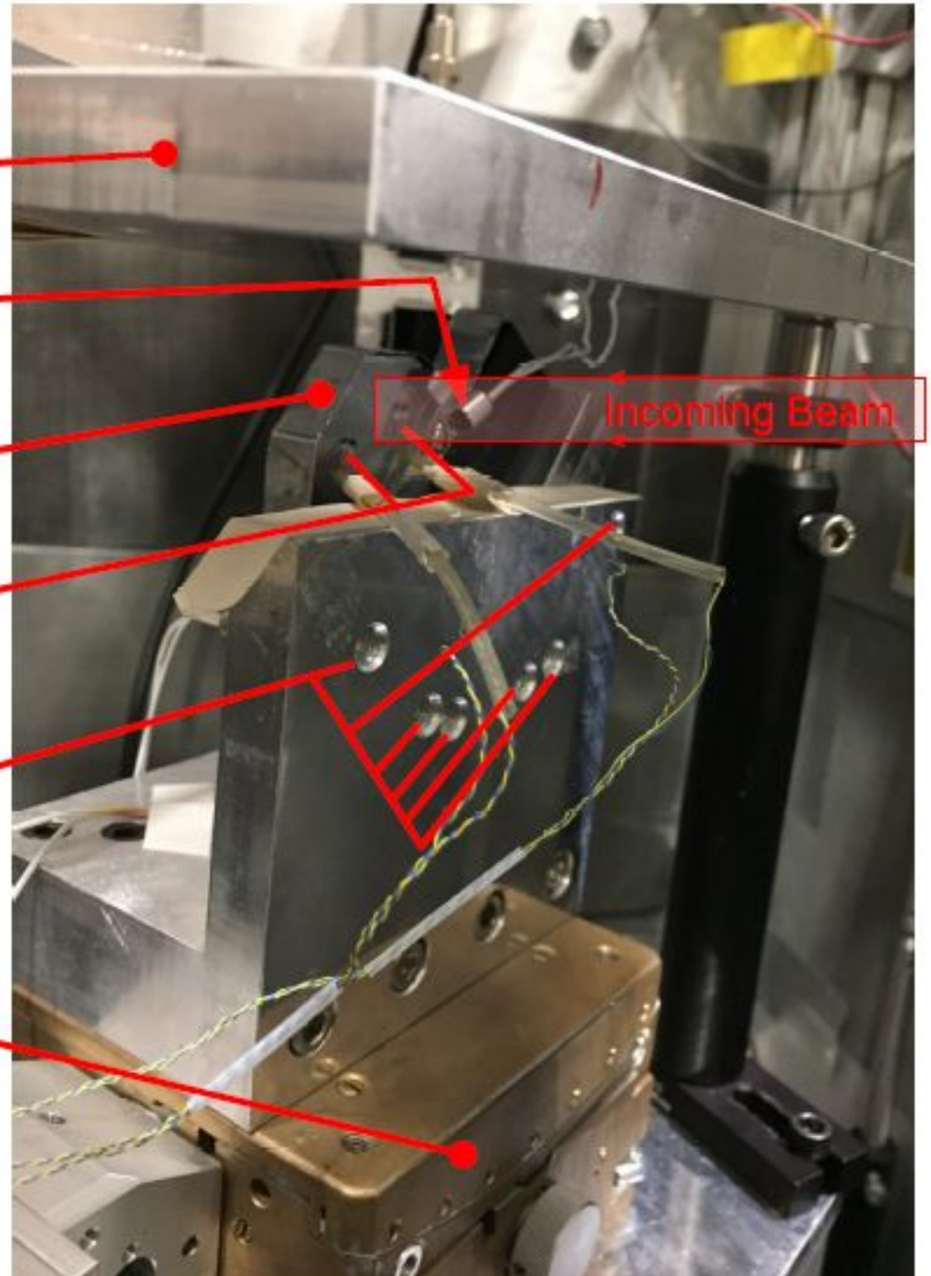

Tilt to change optical thickness, constant λ

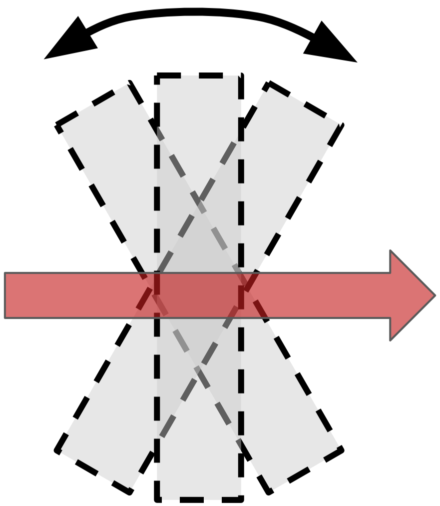

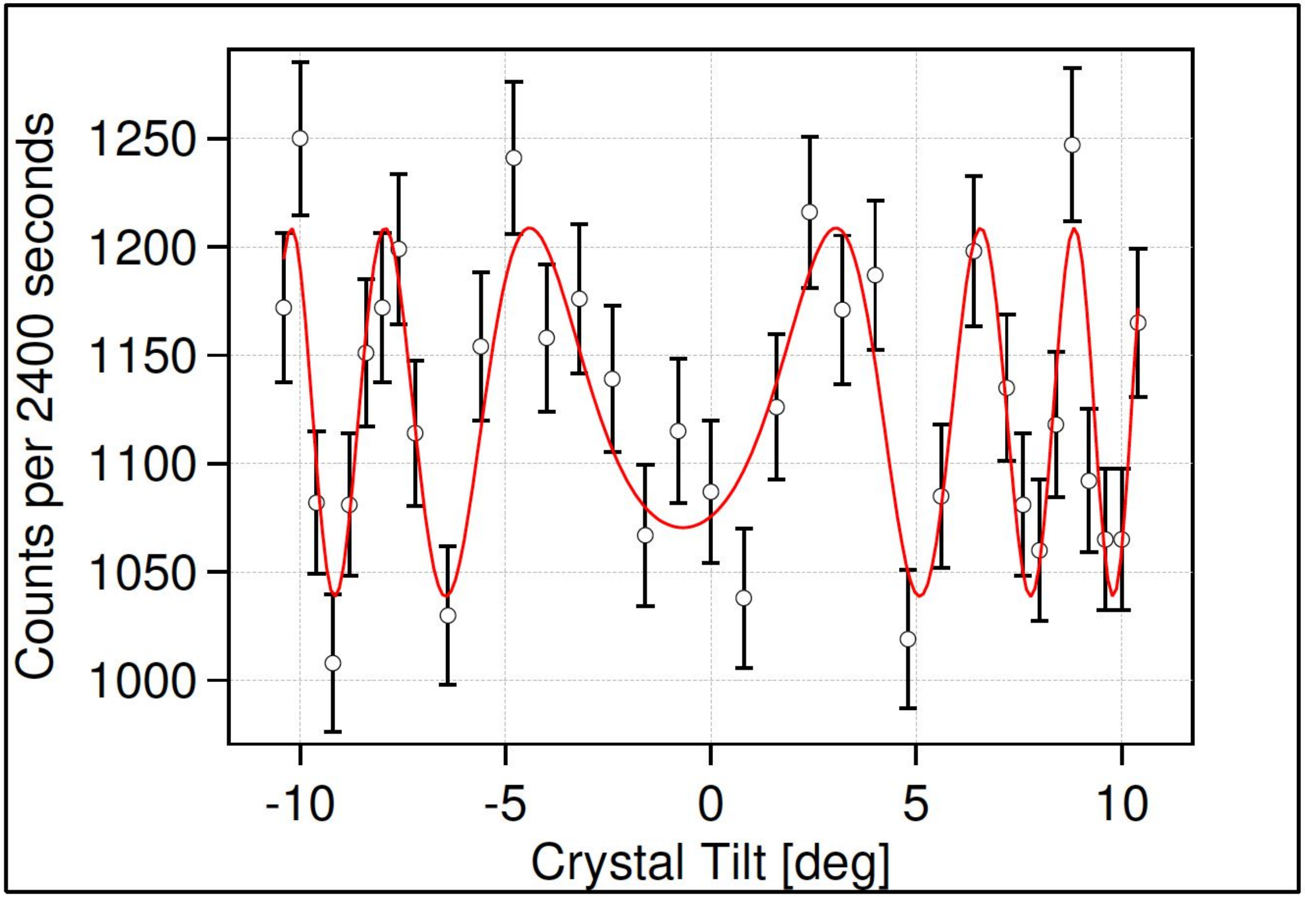

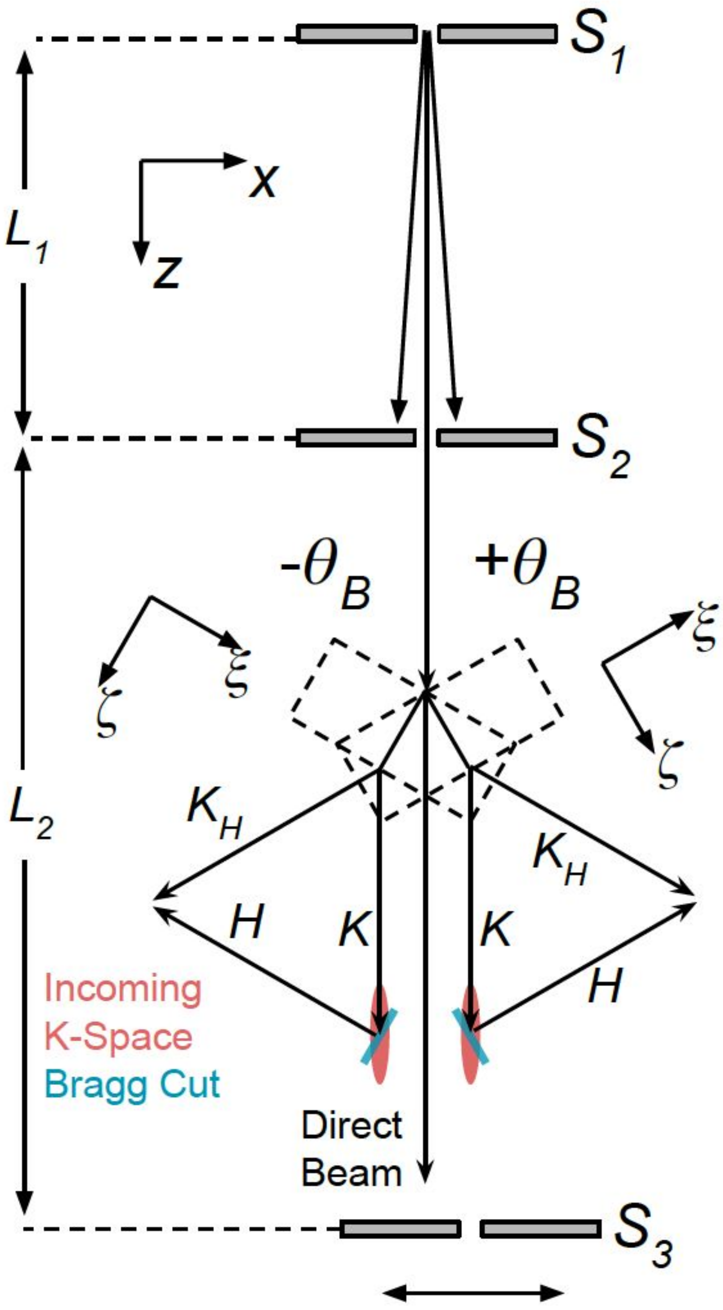

Wavelength

Pendellosung phase shift proportional to tanθ_{B}

Measure at $\pm\theta_{\mathrm{B}}$

Average quadratic in $\delta\theta_{\mathrm{B}}$

Interferometer

In-Out-Out-In to subtract drifts

Repeated at $\pm\theta_B$ to measure wavelength in-situ

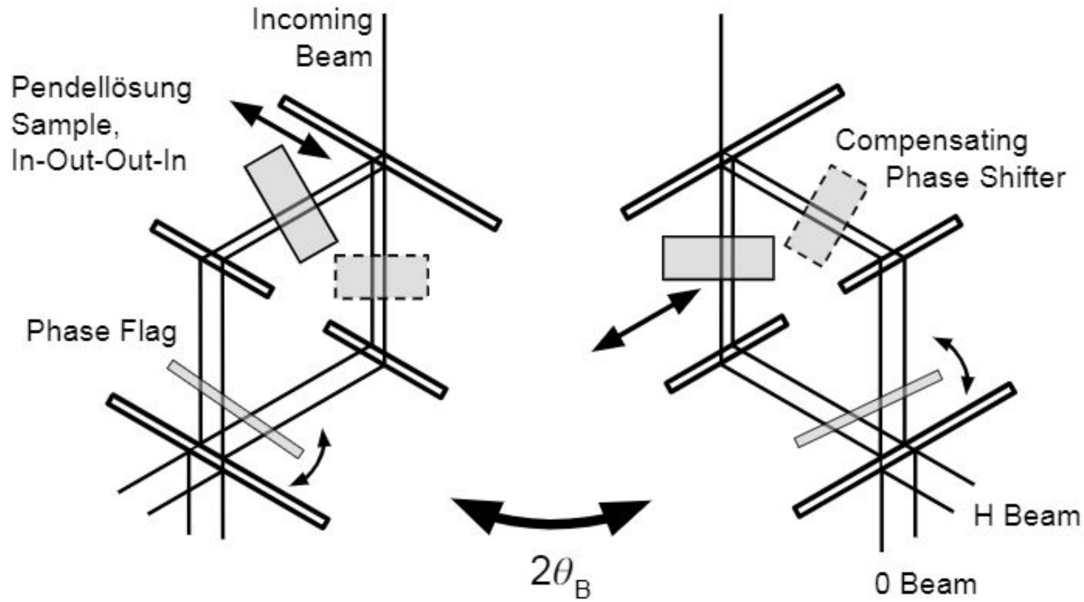

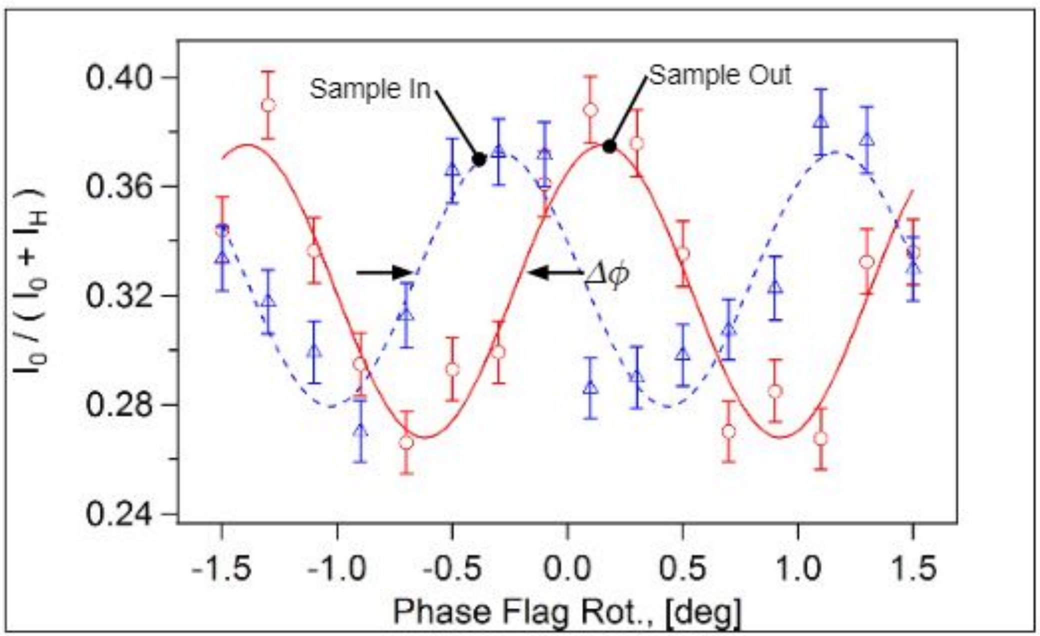

Phase Shift and Drifts

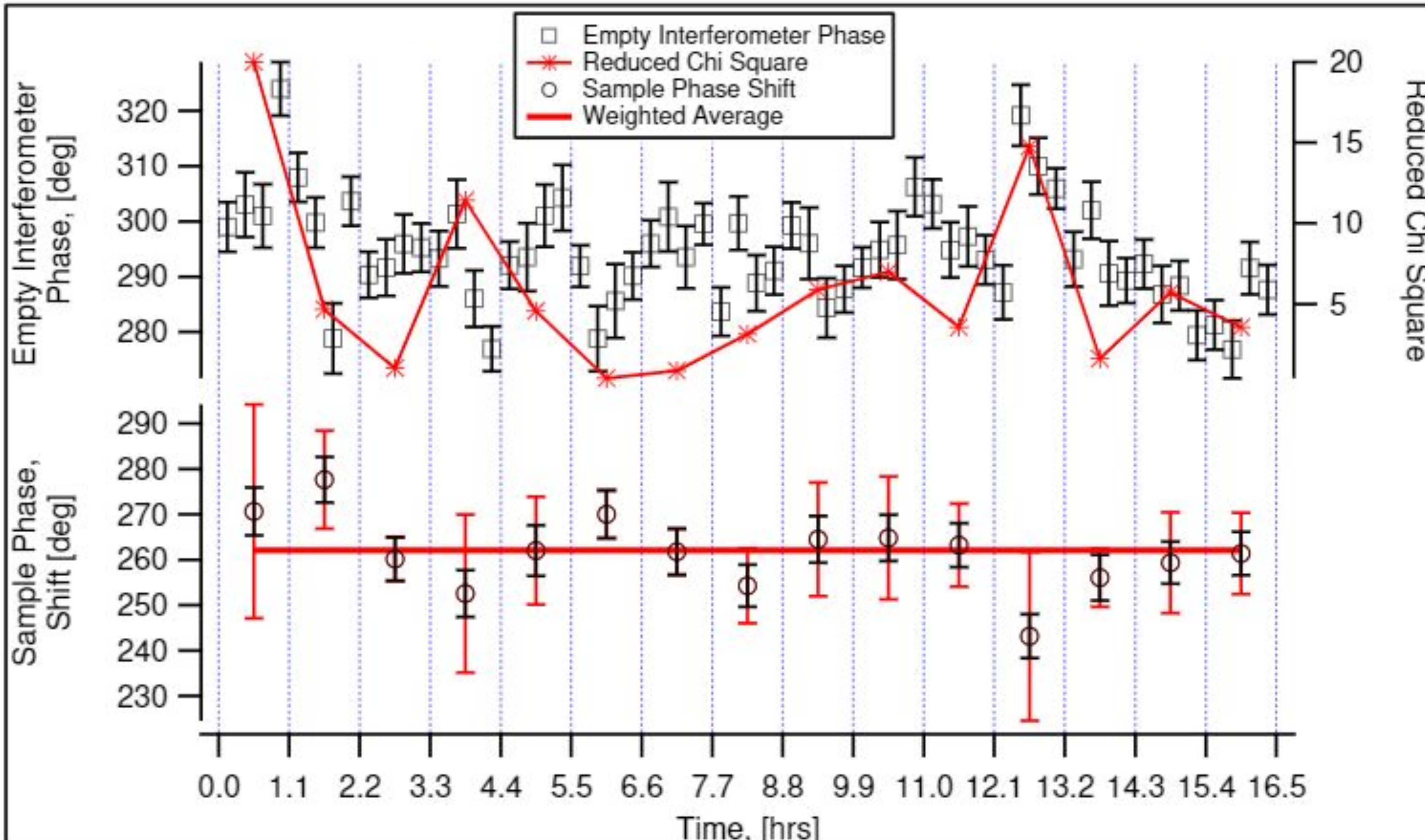

Preliminary Results

hkl	$b(Q)/b(0)-1$	Unc. Stat.	Unc. Sys.	Unc. Total
(111)	-0.011 084	0.000 038	0.000 040	0.000 055
(220)	-0.030 216	0.000 059	0.000 036	0.000 069
(400)	-0.060 559	0.000 080	0.000 051	0.000 095

hkl	$f_{x\text{-ray}}$	b(Q)/b(0)-1
111	10.6298(5)	-0.01094(20) **-0.011084(55)**
220	8.4179(6)	**-0.030216(69)**
311	7.7134(10)	
400	7.0293(4)	**-0.060559(95)**
331	6.7571(9)	
422	6.1382(5)	
333	5.8041(6)	
⋮	⋮	
753	2.5508(29)	
⋮	⋮	
880	1.5514(18)	

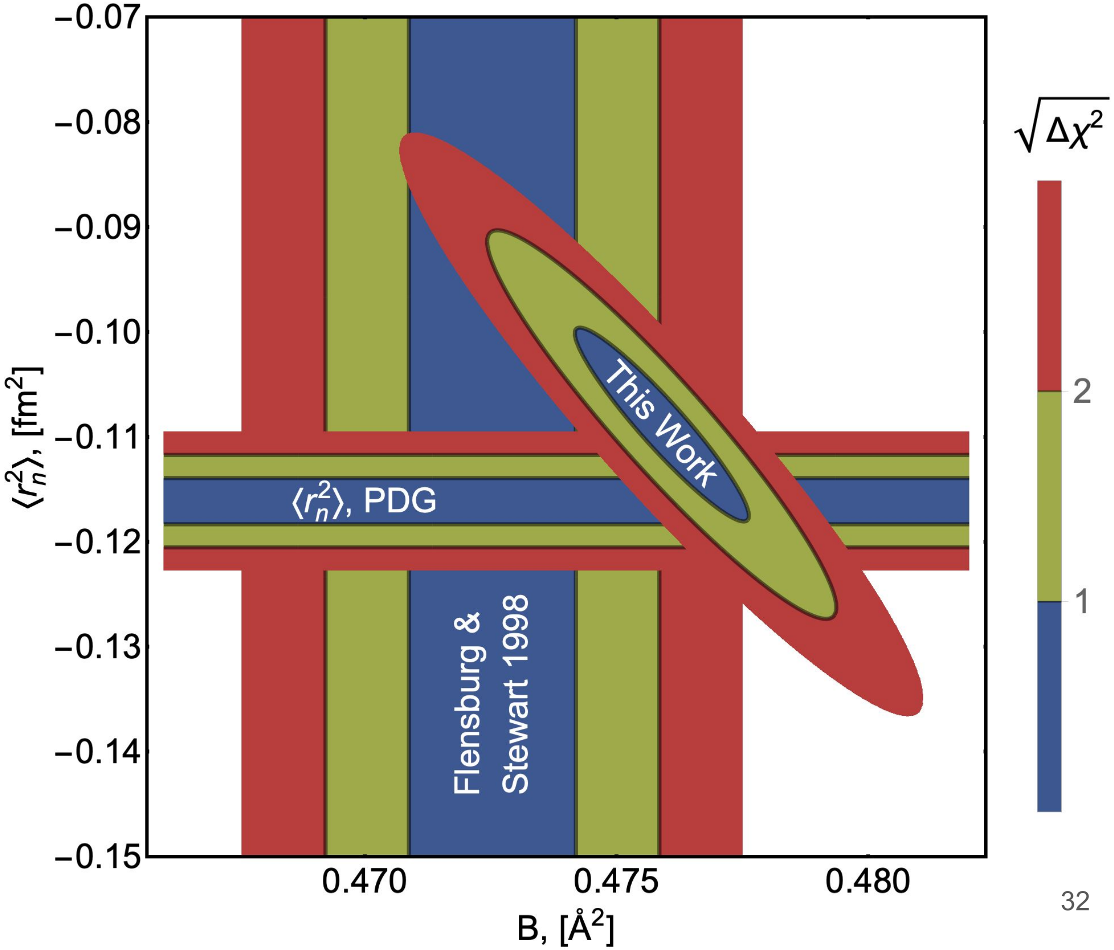

Neutron Charge Radius

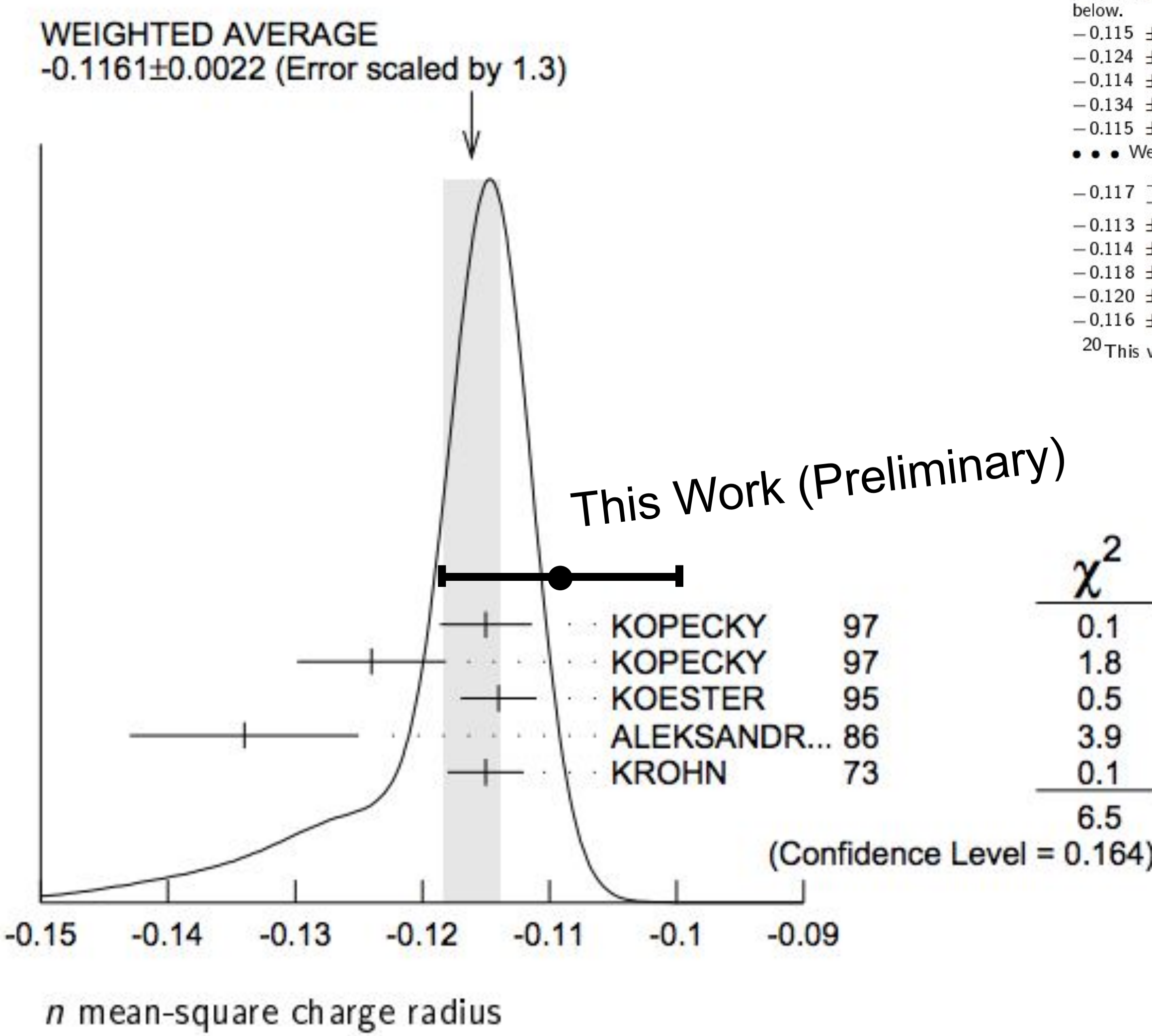

n MEAN-SQUARE CHARGE RADIUS

The mean-square charge radius of the neutron, $\langle r_n^2 \rangle$, is related to the neutron-electron scattering length b_{ne} by $\langle r_n^2 \rangle = 3(m_e a_0/m_n) b_{ne}$, where m_e and m_n are the masses of the electron and neutron, and a_0 is the Bohr radius. Numerically, $\langle r_n^2 \rangle = 86.34\ b_{ne}$, if we use a_0 for a nucleus with infinite mass.

VALUE (fm^2)	DOCUMENT ID		COMMENT
−0.1161±0.0022 OUR AVERAGE	Error includes scale factor of 1.3. See the ideogram below.		
−0.115 ±0.002 ±0.003	KOPECKY	97	ne scattering (Pb)
−0.124 ±0.003 ±0.005	KOPECKY	97	ne scattering (Bi)
−0.114 ±0.003	KOESTER	95	ne scattering (Pb, Bi)
−0.134 ±0.009	ALEKSANDR...	86	ne scattering (Bi)
−0.115 ±0.003	[20] KROHN	73	ne scattering (Ne, Ar, Kr, Xe)
• • • We do not use the following data for averages, fits, limits, etc. • • •			
$-0.117\ ^{+0.007}_{-0.011}$	BELUSHKIN	07	Dispersion analysis
−0.113 ±0.003 ±0.004	KOPECKY	95	ne scattering (Pb)
−0.114 ±0.003	KOESTER	86	ne scattering (Pb, Bi)
−0.118 ±0.002	KOESTER	76	ne scattering (Pb)
−0.120 ±0.002	KOESTER	76	ne scattering (Bi)
−0.116 ±0.003	KROHN	66	ne scattering (Ne, Ar, Kr, Xe)

[20] This value is as corrected by KOESTER 76.

Preliminary Limits

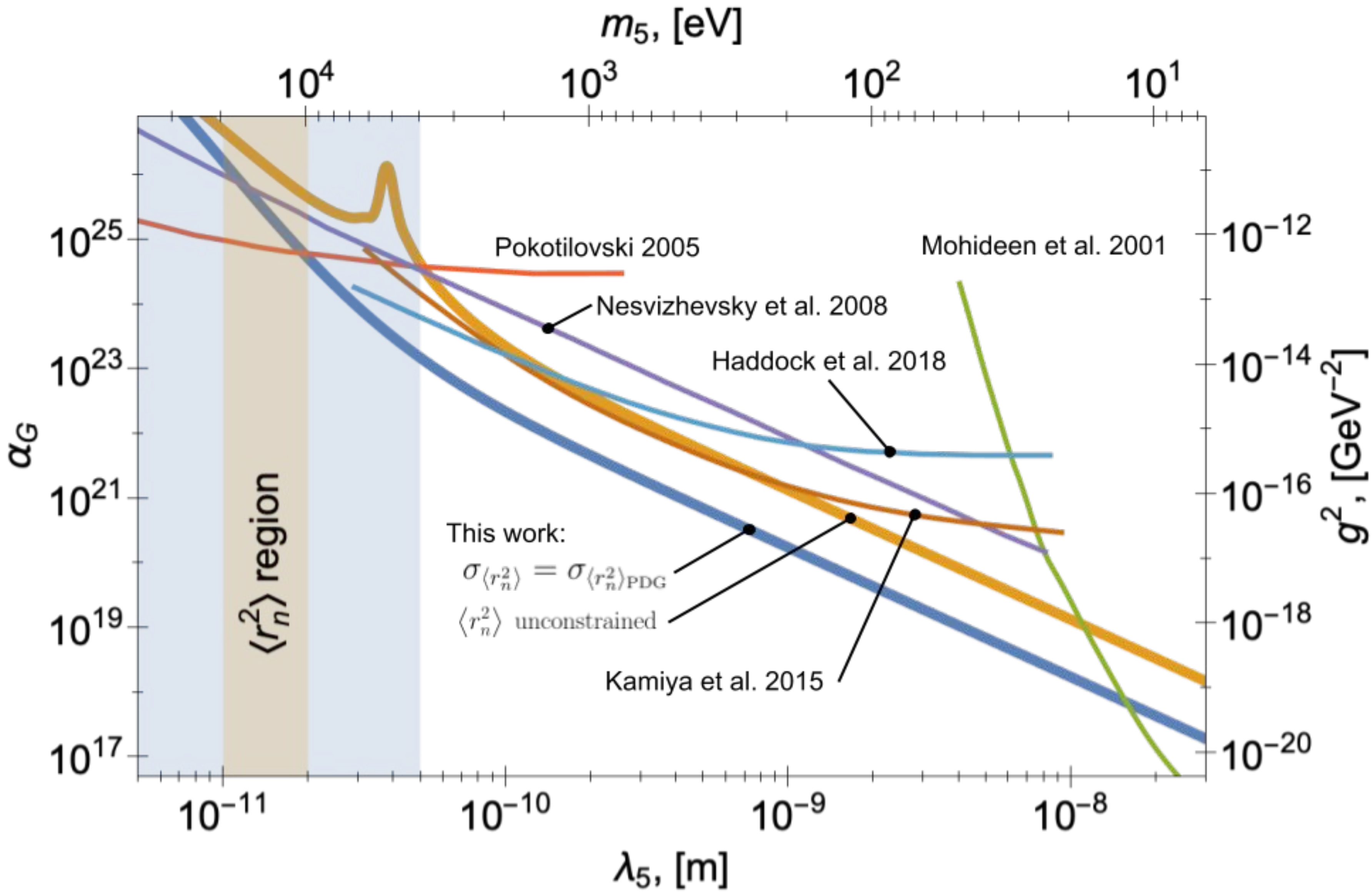

Length Scales and Atomic Form Factors

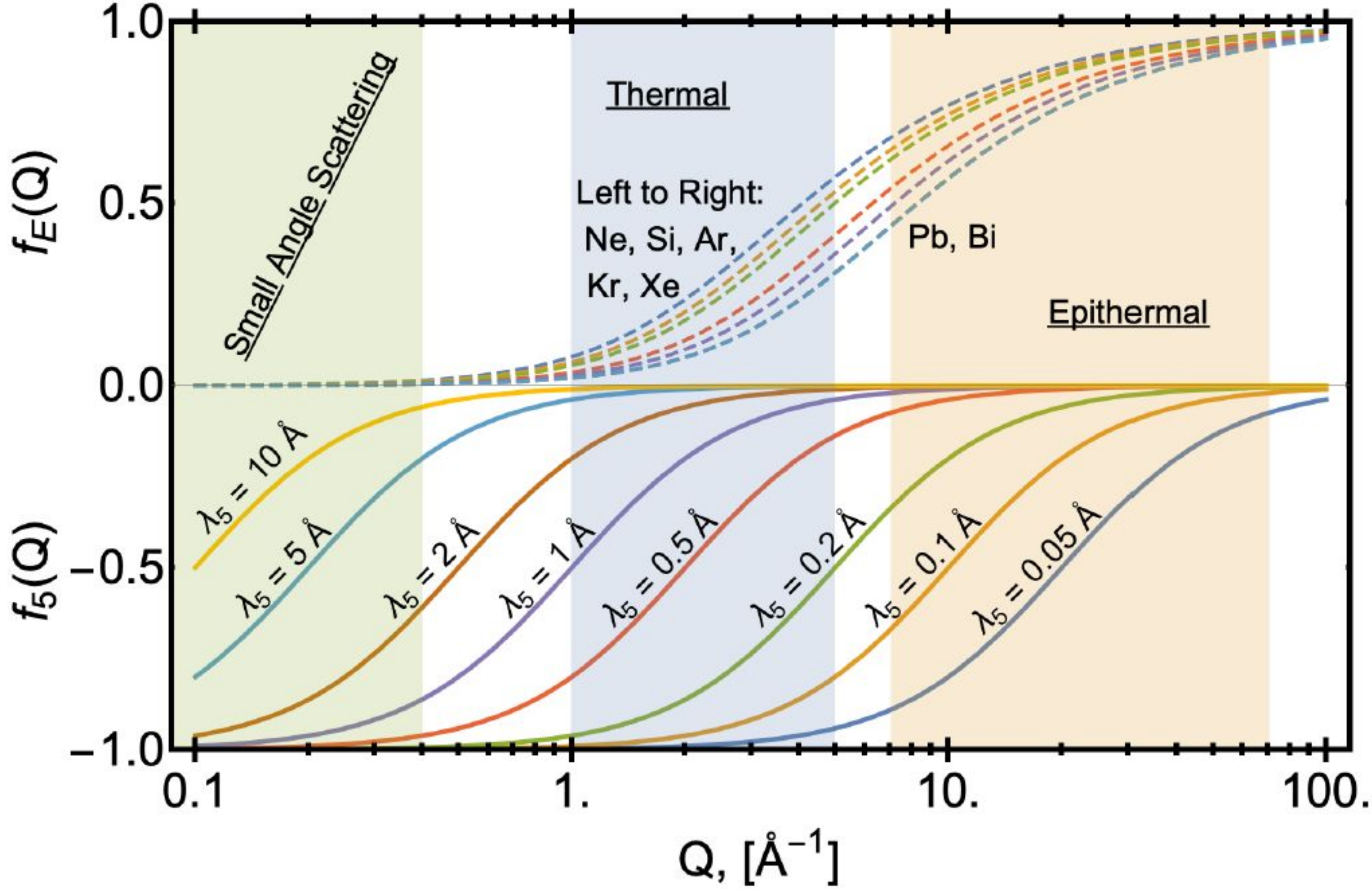

Uncertainty Budget Pendellosung

Source	Uncertainty	$\Delta\phi_P$ (deg)	$\sigma_P/\phi_P \times 10^{-5}$	hkl
S_3 Translation	10 μm	0.0	0.5	111
		1.1	0.4	220
		2.9	0.3	400
Bragg Stage, θ_B	3×10^{-4} deg		1.0	111
			0.8	220
			1.6	400
Temperature Gradient, $p_T^2/6$	0.1×10^{-5}	0.2	0.1	111
	0.2×10^{-5}	0.4	0.2	220
	2.1×10^{-5}	3.7	2.1	400
Absolute Temperature	0.20 K	-1.0	0.7	111
	0.06 K	-1.0	0.6	220
	0.08 K	3.2	1.5	400
Crystal Profile	0.14 μm	1.4	1.4	111
Anharmonic Correction, $f_{\text{anh}}(hkl)$	1×10^{-5}	2.9	1.0	111
Total Sys.			2.2	111
			1.1	220
			3.1	400
$\boldsymbol{\phi_P}$**, Stat.**	2.6 deg		2.5	111
	3.3 deg		5.4	220
	6.3 deg		7.8	400
Total			**3.0**	111
			5.5	220
			8.4	400

Uncertainty Budget Interferometer

Source	Uncertainty	$\Delta\phi_I$ (deg)	$\sigma_I/\phi_I \times 10^5$	hkl
Crystal Translation	1 mm		2.4	111
			2.6	220
			3.8	400
Bragg Stage, θ_B	3×10^{-4} deg		0.7	All
Air Scattering, ϕ_{air}	0.8 deg	105.3 deg	1.6	All
Thermal phase, ϕ_{therm}	0.9 deg	0.6 deg	1.7	All
Total Sys.			3.5	111
			3.5	220
			4.5	400
$\boldsymbol{\phi_I}$**, Stat.**	1.5 deg		2.9	111
	1.5 deg		2.9	220
	1.8 deg		3.5	400
Total			**4.4**	111
			4.5	220
			5.7	400

Future and Ongoing Work

Repeat the experiment with germanium (Takuhiro Fujiie)

Higher-order structure factors

- Valuable to crystal dynamics, neutron charge radius, and fifth force searches

Global analysis of charge radius measurements for better separation of atomic and fifth force form factors (similar to Zimmer & Kaiser 2006)

Neutron interferometer with position-sensitive detector

Pendellosung on a pulsed Beam (Itoh et al 2018)

Pendellosung as a function of temperature

Thank You!


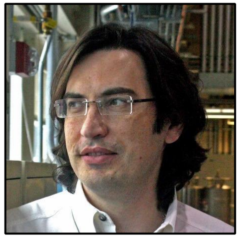
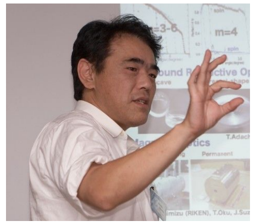




NCSU:
Albert Young
Robert Valdillez

NIST:
Michelle Jamer
Michael Huber
Albert Henins
M. Arif

Nagoya:
Hirohiko Shimizu
Katsuya Hirota
Masaaki Kitaguchi
Tomoki Yamamoto
Takuhiro Fujiie
Masaya Najaki

RIKEN:
Yutaka Yamagata
Takuya Hosobota
Masahiro Takeda

Tulane:
Robert Haun

Waterloo:
Dmitry Pushin
Ivar Taminiau

Special Thanks:
Sam Werner

Borrmann Fan

Edges of the Borrmann fan are detuned from the exact Bragg condition

Pendellosung must be measured at the center of the Borrmann fan

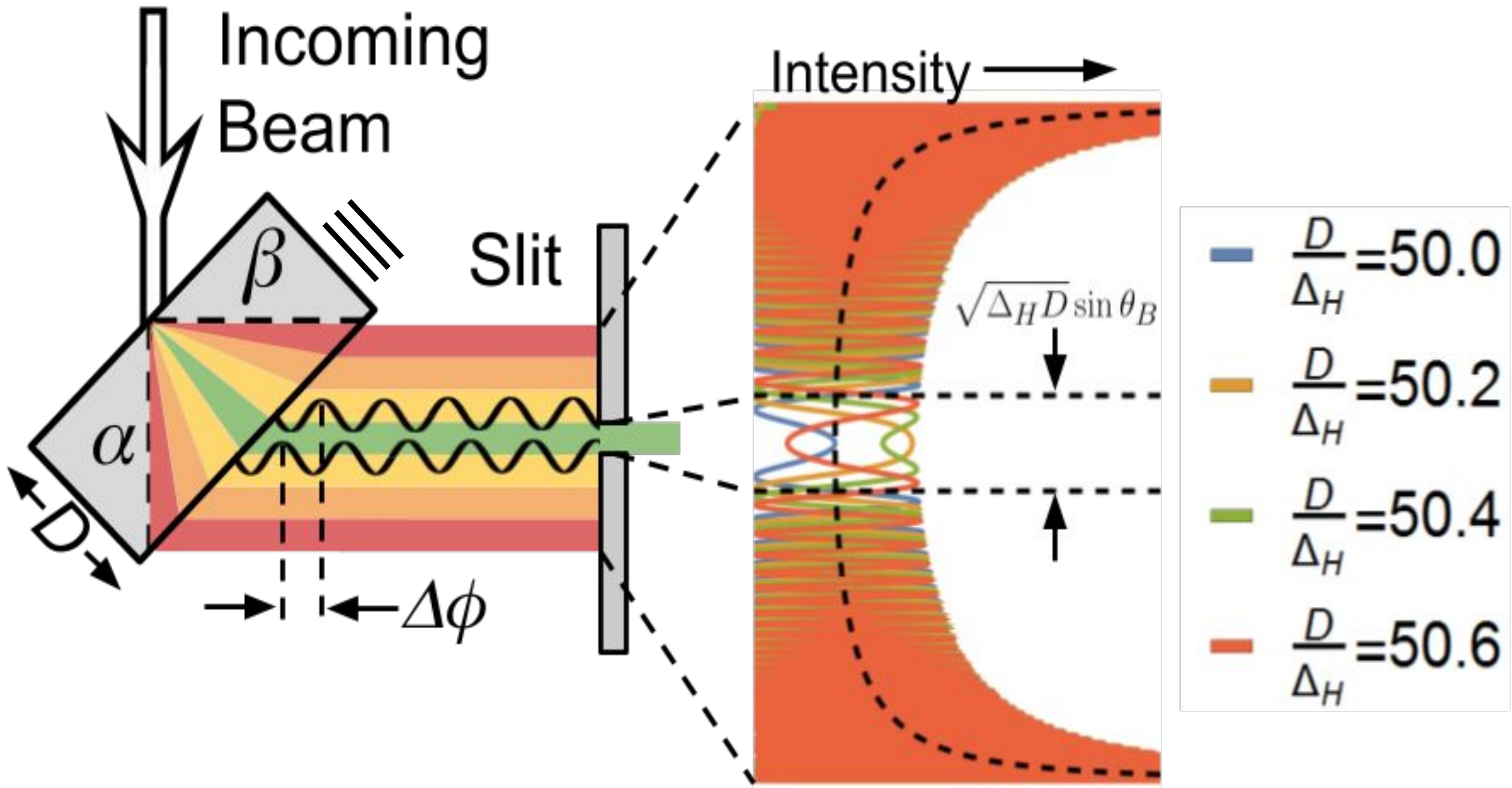

Beam Profiles

Systematic uncertainty associated with different interrogation volumes of the neutron interferometer and pendellosung beam

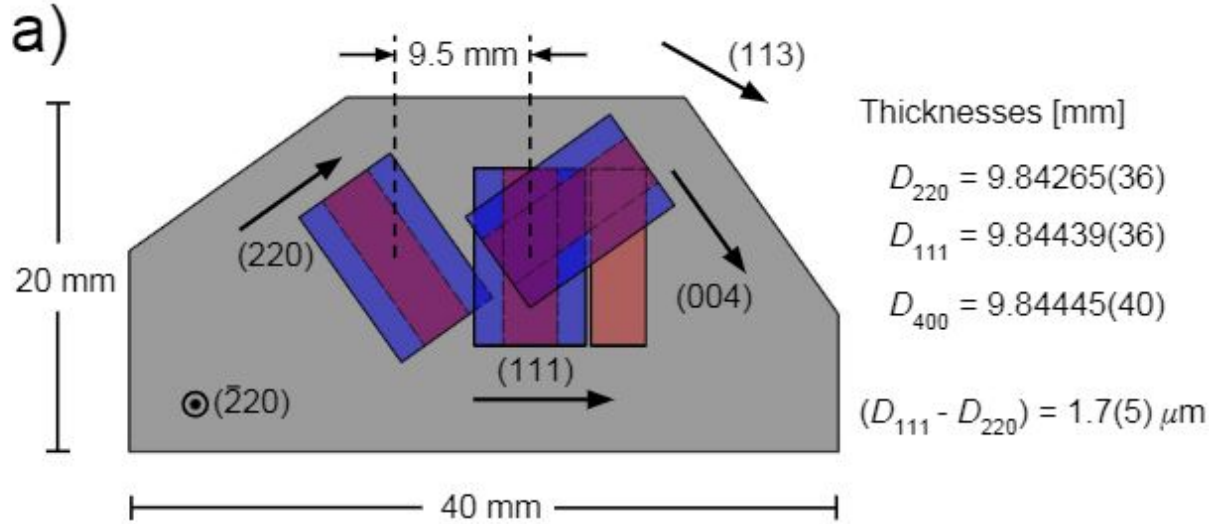

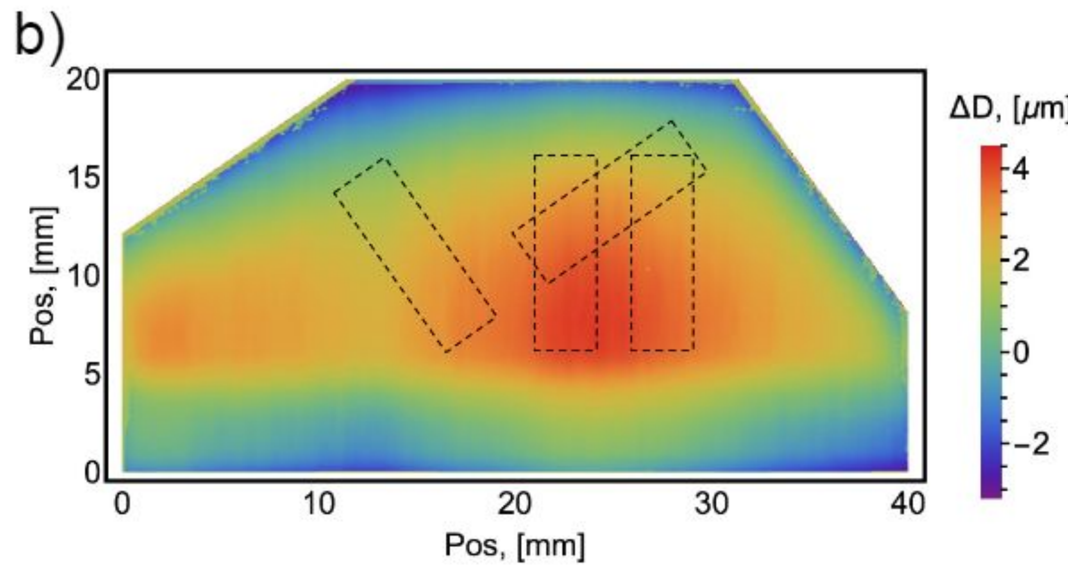

Pendellosung

Length domain

Two state system -
momentum directions

Bragg misalignment

$$\vec{K}\cdot\vec{H}=\left(-\frac{1}{2}\vec{H}+\delta\vec{K}\right)\cdot\vec{H}$$

Pendellosung length

Strength of potential

$$\Delta_H=\pi\frac{H\cot\theta_B}{v_H}$$

Time Sinusoidal (NMR)

Time domain

Two state system -
energy levels

Resonance condition

$$\omega=\frac{E_2-E_1}{\hbar}+\delta\omega$$

Rabi flopping

Strength of potential

Anharmonic Contribution

The “nice” functional for of the DWF assumes a harmonic lattice potential

The different atoms with opposite bonding parities see opposite cubic contribution to interatomic potential

Cubic contribution is required for thermal expansion

- Silicon’s negative coefficient of thermal expansion at low temperatures makes it especially interesting

$$\mathcal{H} = \frac{p_i^\alpha p_i^\alpha}{2m_i} + \frac{1}{2}\Phi_{ij}^{\alpha\beta} u_i^\alpha u_j^\beta + \frac{1}{3!}\Psi_{ijk}^{\alpha\beta\gamma} u_i^\alpha u_j^\beta u_k^\gamma$$

Cubic Terms in Silicon

$$\left|\left\langle \sum_v e^{i\vec{H}\cdot\vec{x}_v} \right\rangle\right| = \begin{cases} \sqrt{32}e^{-W}\left[1 - T_a(hkl)\right], & h+k+l = 4n-1 \\ & h,k,l \in \mathrm{Odd} \\ \sqrt{32}e^{-W}\left[1 + T_a(hkl)\right], & h+k+l = 4n+1 \\ & h,k,l \in \mathrm{Odd} \\ 8e^{-W}, & h+k+l = 4n \\ & h,k,l \in \mathrm{Even} \\ 8e^{-W}T_a(hkl), & h+k+l = 4n\pm 2 \\ & h,k,l \in \mathrm{Even} \end{cases}$$

$$T_a(hkl) = \frac{1}{6}\left\langle \left(\vec{H}\cdot\vec{u}\right)^3 \right\rangle = \left(\frac{B}{4\pi a}\right)^3 \frac{\beta}{k_B T} hkl \simeq (3\times 10^{-5})hkl$$

$$\beta = \Psi_{iii}^{xyz}$$

Forbidden Reflections

One class of forbidden reflections is nonzero due to

Bonding Electrons

Anharmonic atomic motion

Measured using absolute reflectivity as a function of temperature

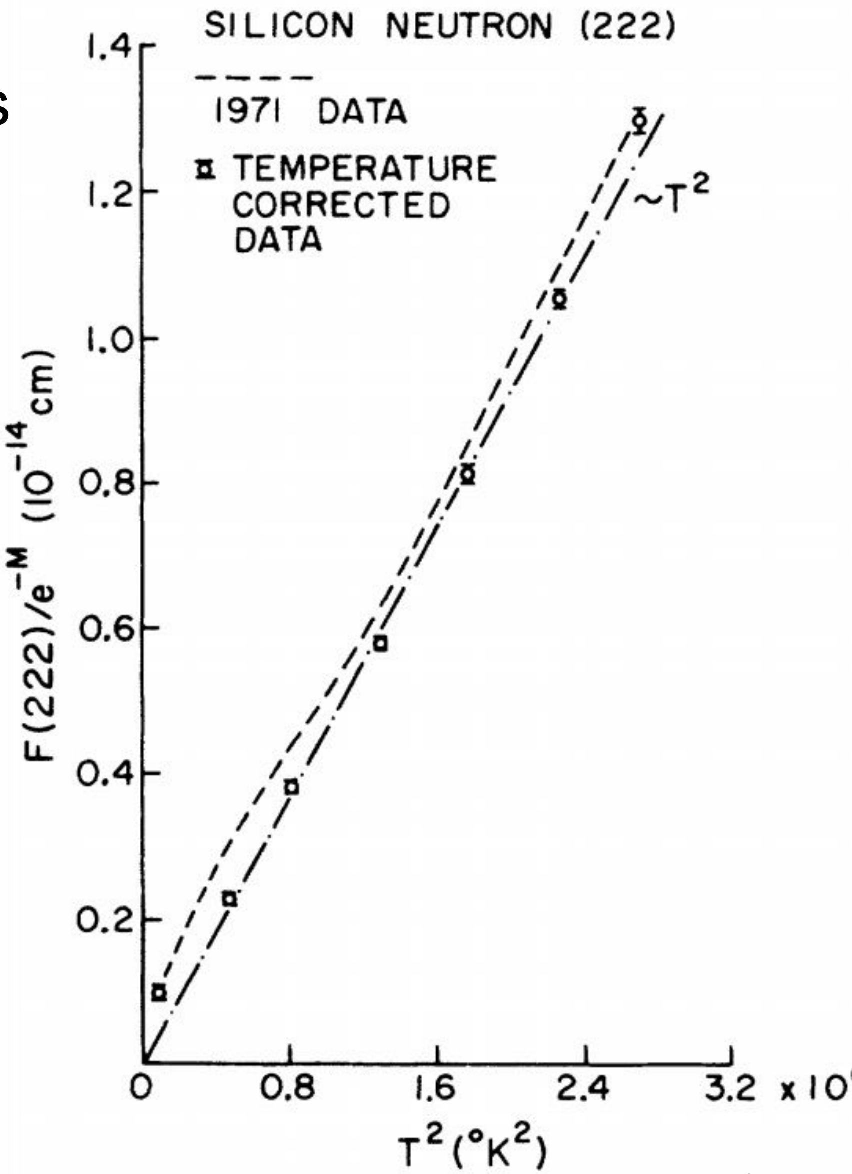

Roberto et al. 1974

Forbidden Reflections

One class of forbidden reflections is nonzero due to

Bonding Electrons

Anharmonic atomic motion

Measured using absolute reflectivity as a function of temperature

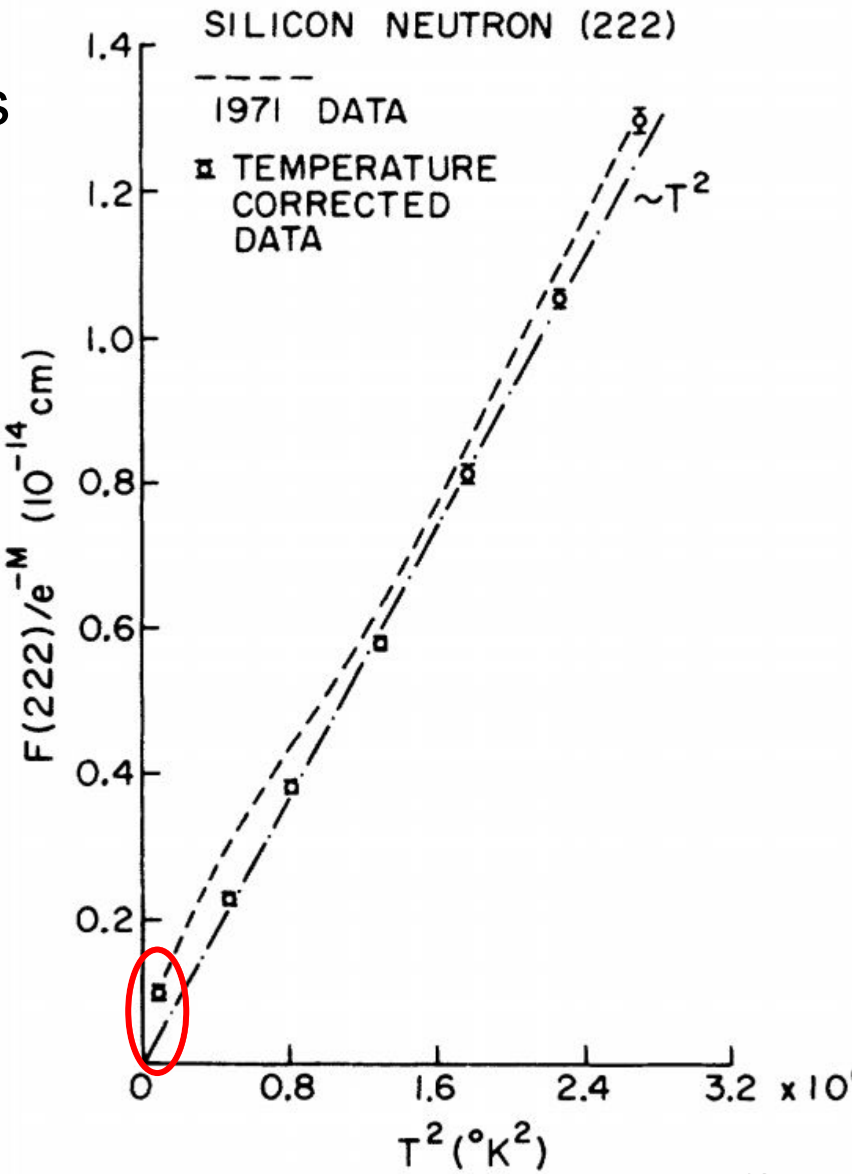

Roberto et al. 1974

Nuclear quantum effect with pure anharmonicity and the anomalous thermal expansion of silicon

D. S. Kim[a,1,2], O. Hellman[a,1], J. Herriman[a], H. L. Smith[a], J. Y. Y. Lin[b], N. Shulumba[c], J. L. Niedziela[d], C. W. Li[e], D. L. Abernathy[f], and B. Fultz[a,2]

[a]Department of Applied Physics and Materials Science, California Institute of Technology, Pasadena, CA 91125; [b]Neutron Data Analysis and Visualization Division, Oak Ridge National Laboratory, Oak Ridge, TN 37831; [c]Department of Mechanical and Civil Engineering, California Institute of Technology, Pasadena, CA 91125; [d]Instrument and Source Division, Oak Ridge National Laboratory, Oak Ridge, TN 37831; [e]Department of Mechanical Engineering, University of California, Riverside, CA 92521; and [f]Quantum Condensed Matter Division, Oak Ridge National Laboratory, Oak Ridge, TN 37831

Edited by Alexi Maradudin, University of California, Irvine, CA and accepted by Editorial Board Member Zachary Fisk December 26, 2017 (received for review May 18, 2017)

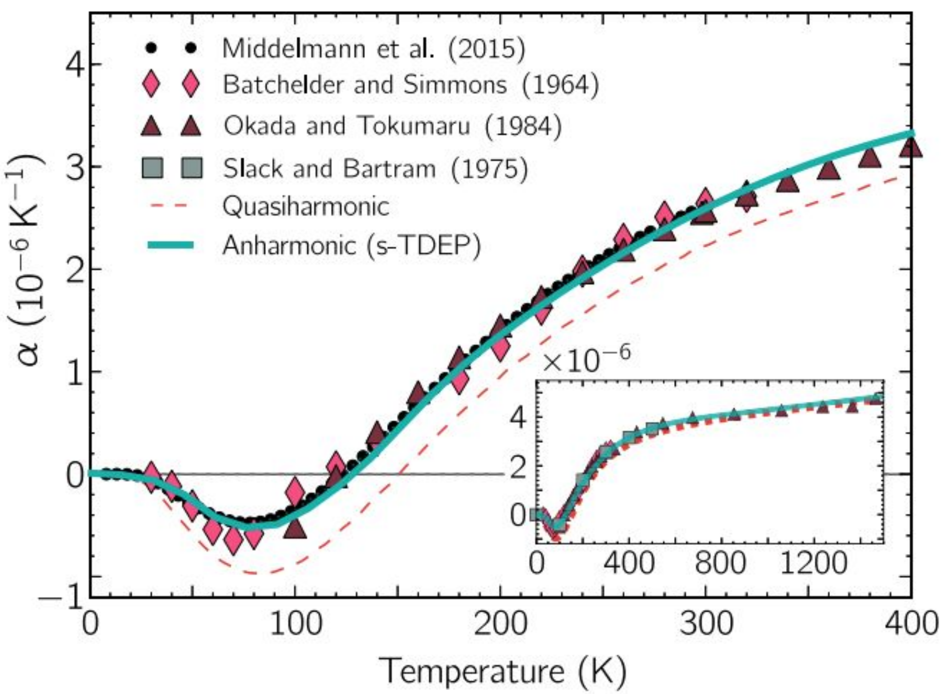

Significance

Silicon has a peculiar negative thermal expansion at low temperature. This behavior has been understood with a "quasiharmonic" theory where low-energy phonons decrease in frequency with volume contraction. We report inelastic neutron scattering measurements of phonon dispersions over a wide range of temperatures. These measurements cast doubt upon quasiharmonic theory, which predicts the wrong sign for most phonon shifts with temperature. Fully anharmonic ab initio calculations correctly predict the phonon shifts and thermal expansion. Crystal structure, anharmonicity, and nuclear quantum effects all play important roles in the thermal expansion of silicon, and a simple mechanical explanation is inappropriate. The quantum effect of nuclear vibrations is also expected to be important for thermophysical properties of many materials.